

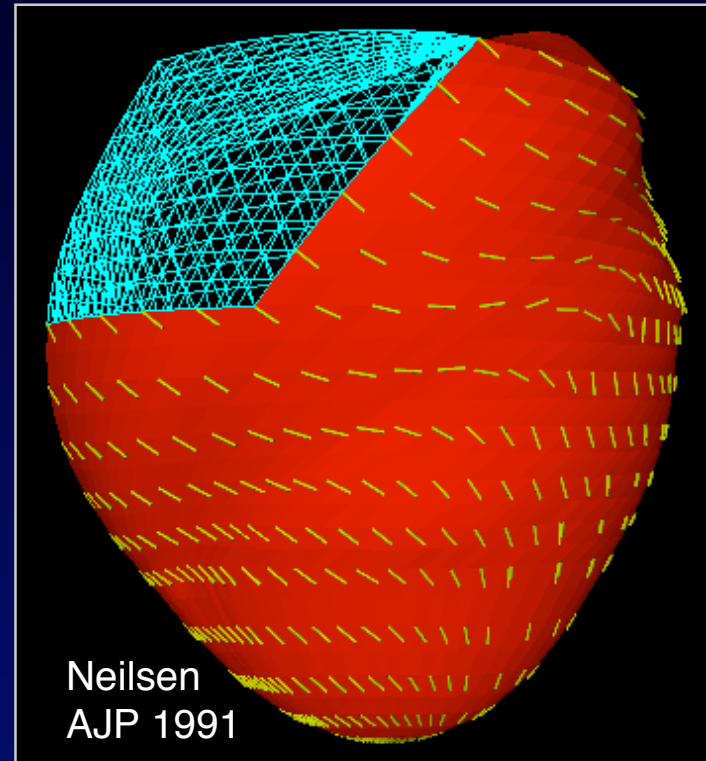
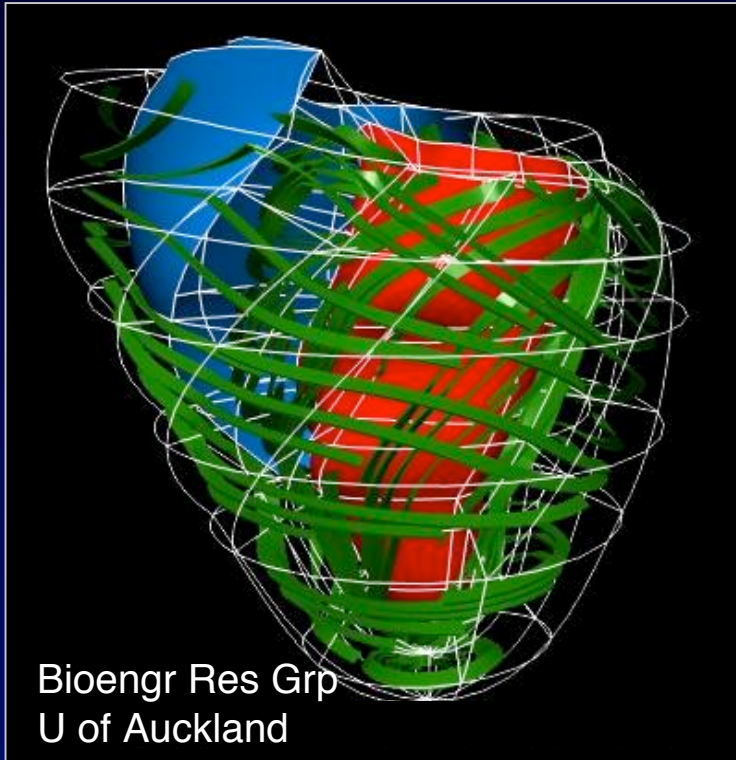
Imaging-Based Structural Models of the Myocardium

Edward Hsu, Ph.D.



Department of Bioengineering
Small Animal Imaging Facility

Myocardial “Functional Anatomy”



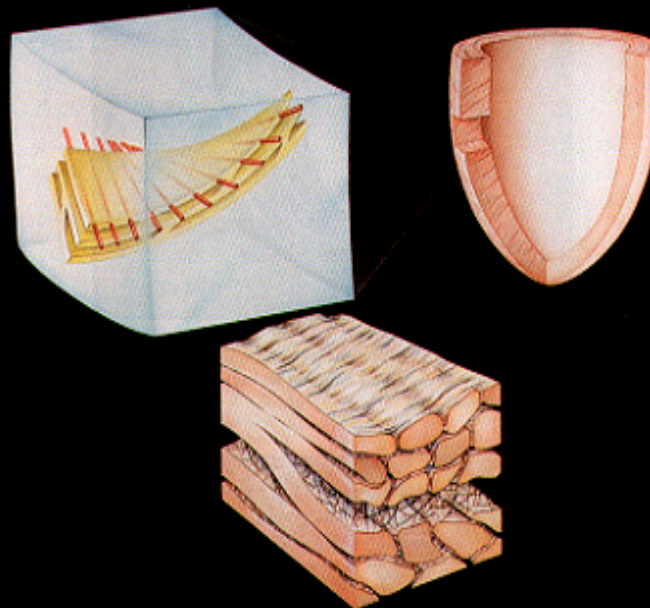
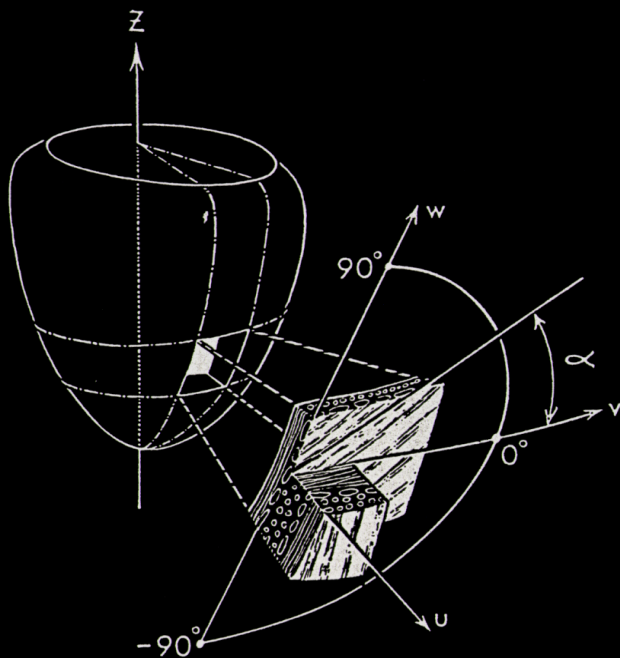
Modeling versus “morphologically accurate” modeling

Tissue Microstructure Histology

Myocardial structures

Fibers

Streeter et al., 1969



Sheets

LeGrice et al. 1995

Histology:

- “gold standard”
- destructive
- labor intensive
- prone to artifacts

Myocardial Structural Models /Atlases

Key Challenges

1. Fiber Orientation Measurement:

- alternative to histology
- suitable for the mouse

2. Statistics:

- inter-species variability
- intra-species variability
- atlas?

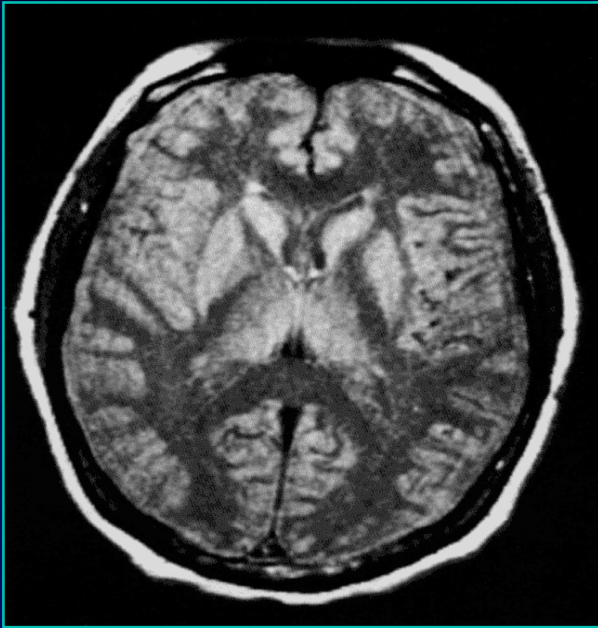
Imaging Based Alternatives

Requirements:

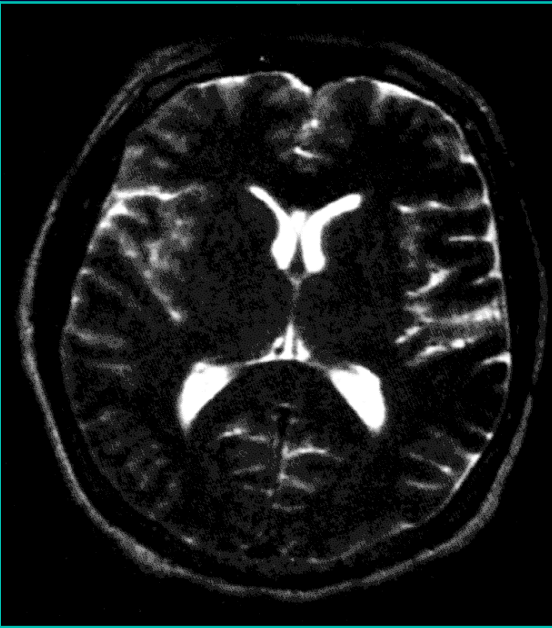
- noninvasive / nondestructive
- in vivo capable
- reasonable resolution
- intrinsic tissue contrast

MR Diffusion Imaging

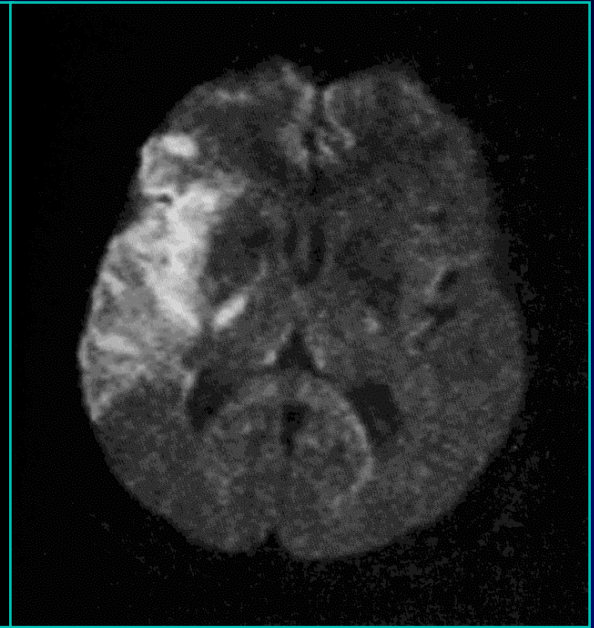
Detection of Early Stroke



PD



T2

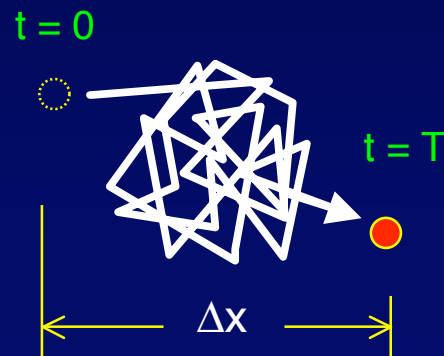
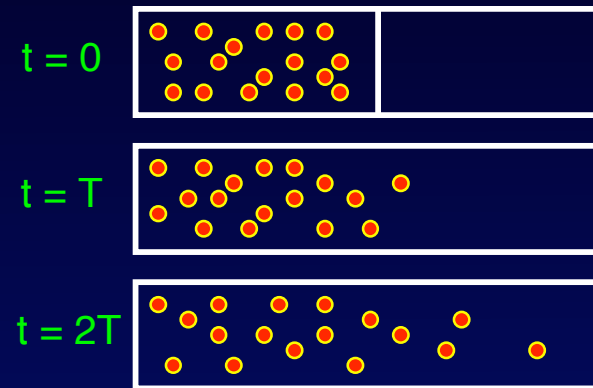


DW

Diffusion is highly sensitive to tissue microstructure!

Diffusion in MRI

Conventional transport:



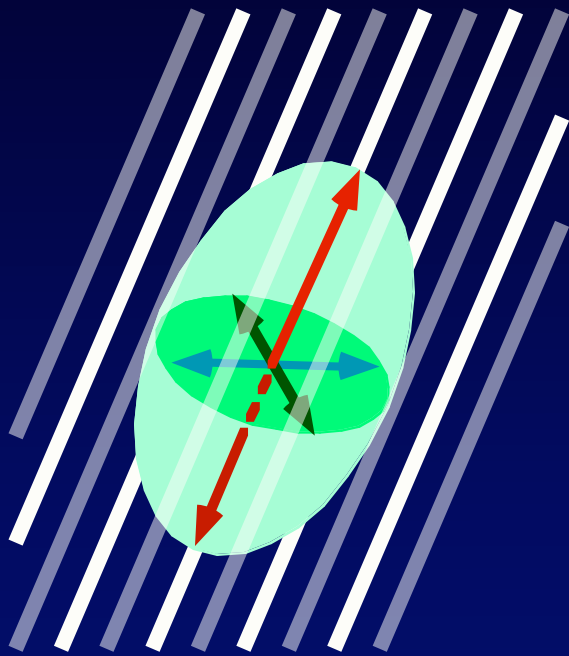
MRI:

- Random translational motion
- Diffusion **in** water versus diffusion **of** water

Diffusion in Anisotropic Tissues

examples:

- brain white matter
- myocardium
- cartilage ...



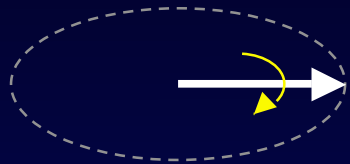
$$\mathbf{D} = \begin{bmatrix} D_{xx} & D_{xy} & D_{xz} \\ D_{xy} & D_{yy} & D_{yz} \\ D_{xz} & D_{yz} & D_{zz} \end{bmatrix}$$

MR diffusion tensor imaging
(MR-DTI)

Overview

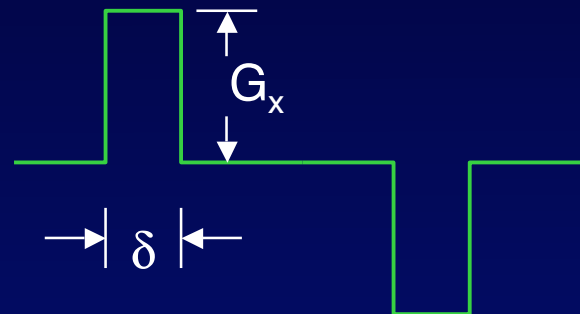
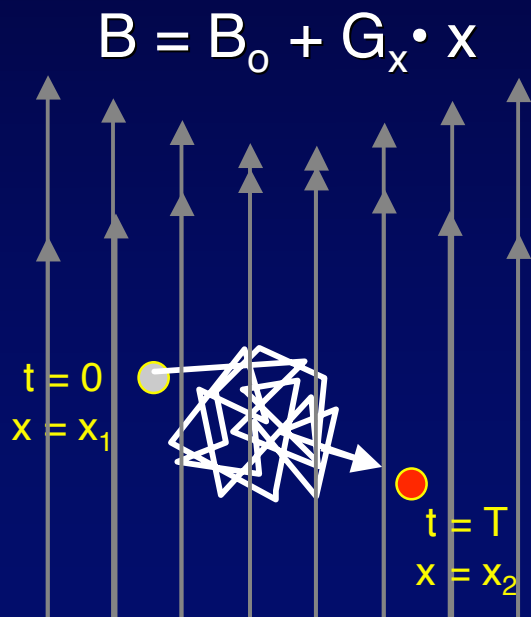
- Principles and Methods of DTI
- Engineering Challenges
- Applications of Cardiac DTI
- Myocardial Structural Models and Atlases

MR Diffusion Encoding



spin precession frequency

$$\omega = \gamma B$$



$$\phi_1 = \gamma \delta G_x x_1$$

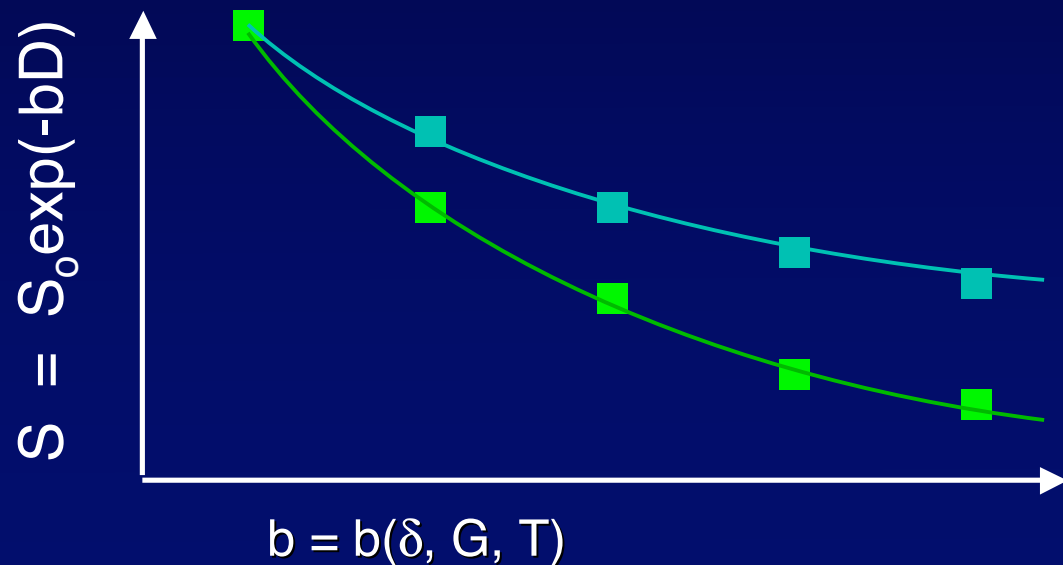
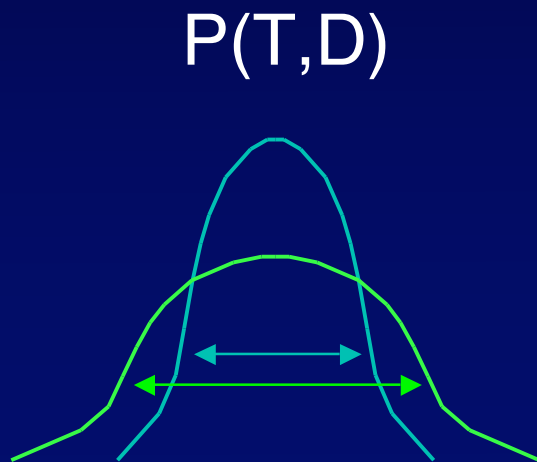
$$\phi_2 = -\gamma \delta G_x x_2$$

$$\left. \begin{array}{l} \phi_1 = \gamma \delta G_x x_1 \\ \phi_2 = -\gamma \delta G_x x_2 \end{array} \right\} \Delta\phi = \gamma \delta G_x \Delta x$$

Diffusion Induced Signal Attenuation

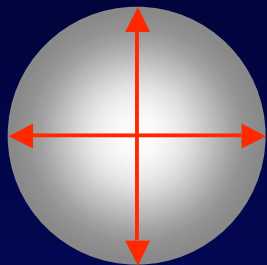
$$S = S_0 \langle \Delta\phi \rangle = S_0 \int \Delta\phi P(T, D) d\phi$$

$$S = S_0 \exp(-bD), \quad b = \gamma^2 \int_0^{TE} \left[\int_0^t G_x(t') dt' \right]^2 dt$$

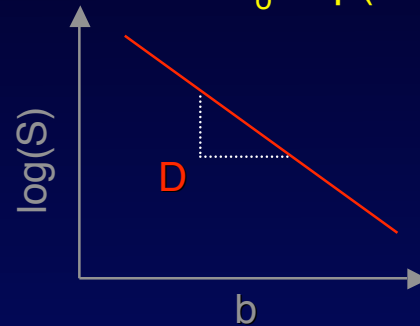


Beyond Isotropic Diffusion

isotropic



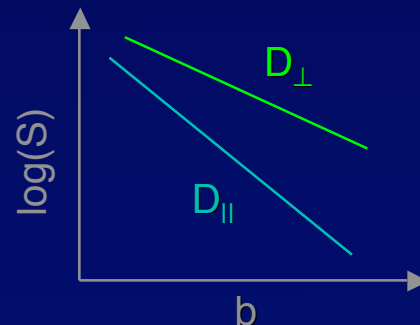
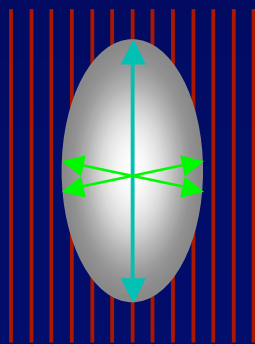
$$S = S_0 \exp(-bD)$$



ADC independent of

$$\mathbf{g} = \begin{bmatrix} g_x \\ g_y \\ g_z \end{bmatrix}$$

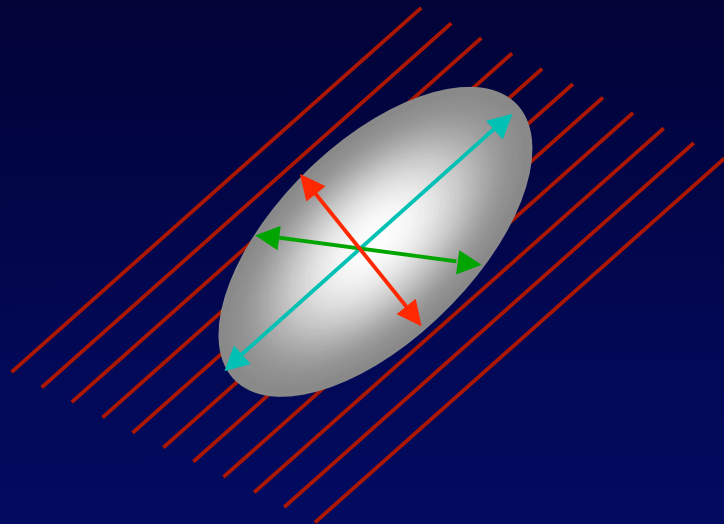
axisymmetric anisotropy



$$\text{ADC} = \mathbf{g}^T \cdot \begin{bmatrix} D_{\perp} & 0 & 0 \\ 0 & D_{\perp} & 0 \\ 0 & 0 & D_{\parallel} \end{bmatrix} \cdot \mathbf{g}$$

$$S = S_0 \exp(-b\mathbf{g}^T \cdot \mathbf{D}_{\Delta} \cdot \mathbf{g})$$

Generalized Anisotropic Diffusion



Rotate \mathbf{G} into local diffusion axes

$$\mathbf{g}' = \mathbf{R} \mathbf{g}$$

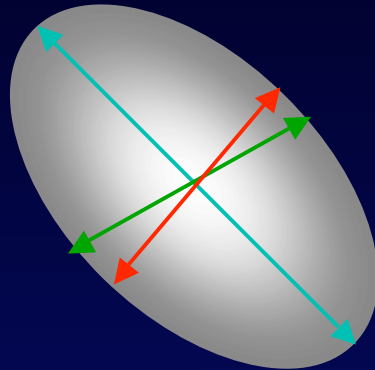
$$\text{ADC} = \mathbf{g}'^T \cdot \mathbf{R}^T \mathbf{D}_{\Delta} \mathbf{R} \cdot \mathbf{g}$$

$$\mathbf{D} = \mathbf{R}^T \mathbf{D}_{\Delta} \mathbf{R} = \begin{bmatrix} D_{xx} & D_{xy} & D_{xz} \\ D_{xy} & D_{yy} & D_{yz} \\ D_{xz} & D_{yz} & D_{zz} \end{bmatrix}$$

DTI strategy:

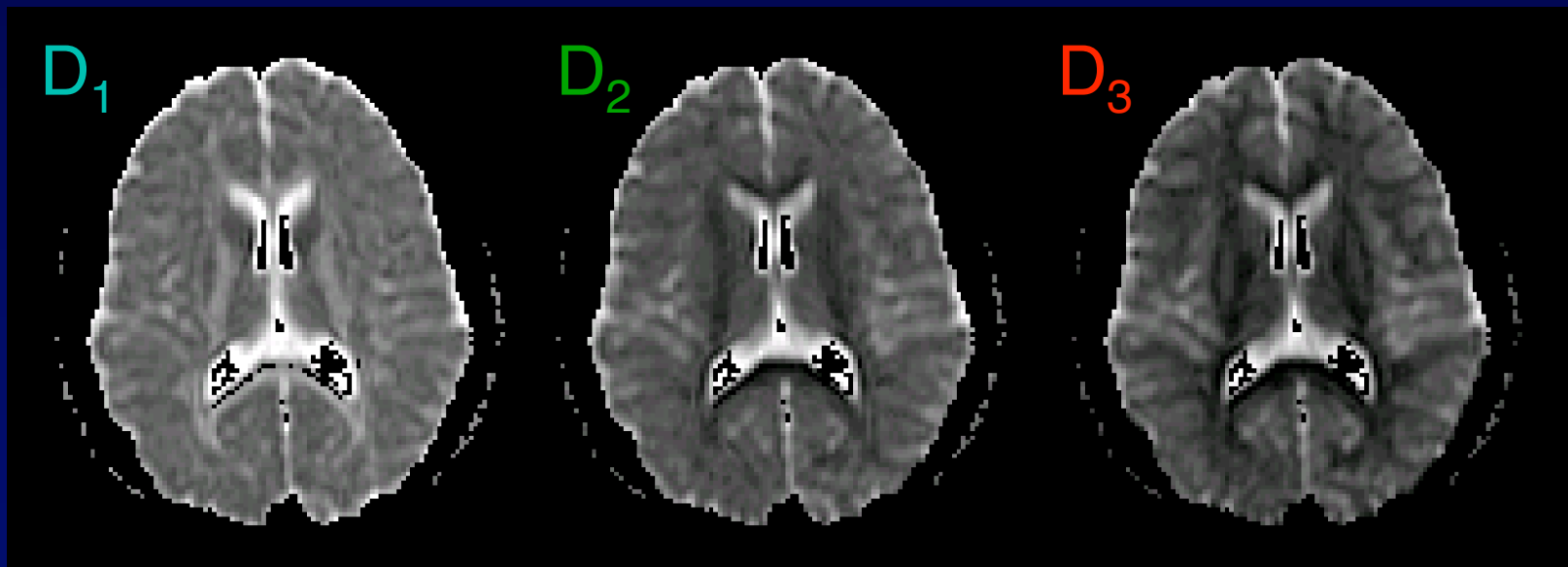
- use \mathbf{g} to probe \mathbf{D}
- encode in at least 6 non-collinear directions
- calculate \mathbf{D} , then diagonalize

Tensor Diagonalization: Eigenvalues



diffusion along principal axes

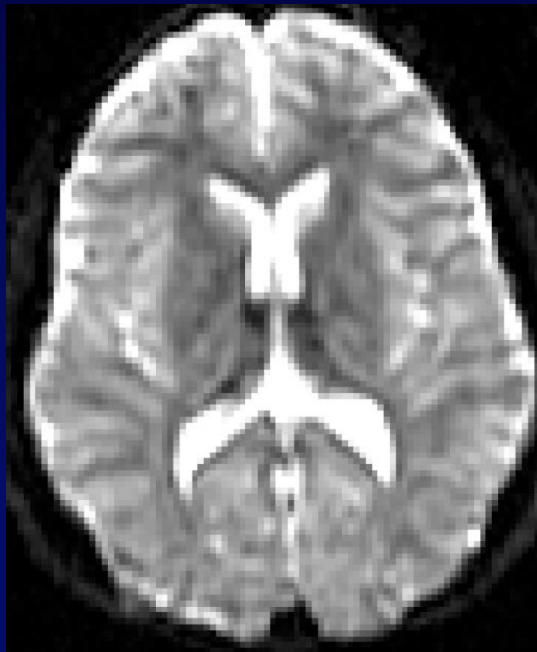
$$D_1 \geq D_2 \geq D_3$$



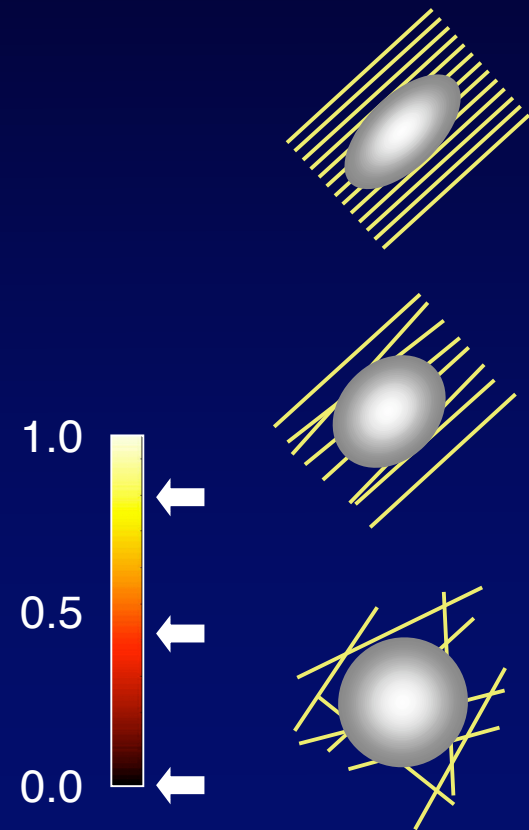
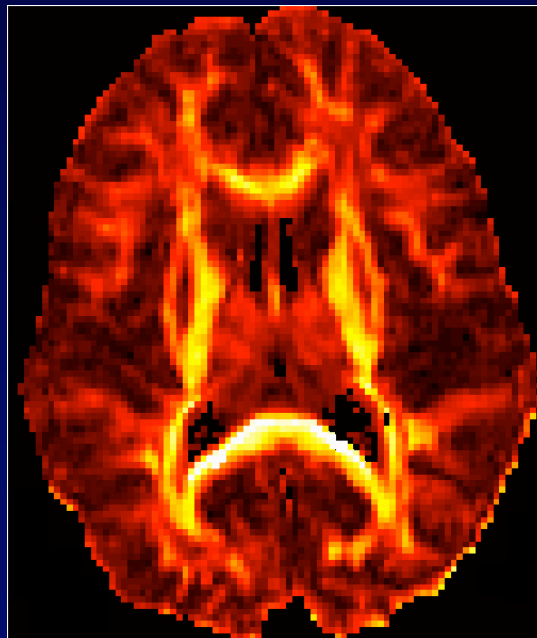
DTI: Scalar Anisotropy Index

Contrast for tissue microstructure

conventional T2

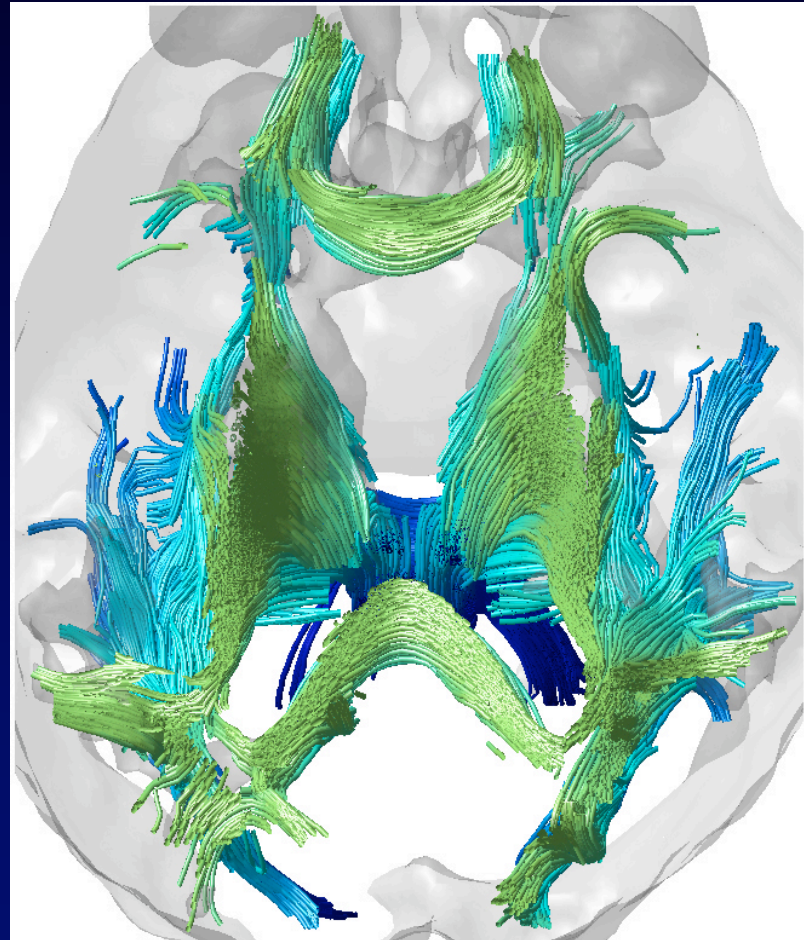
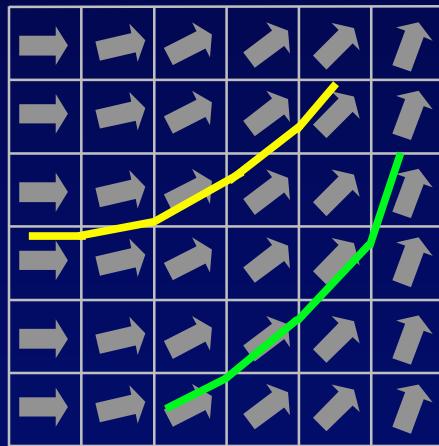


“fractional anisotropy”

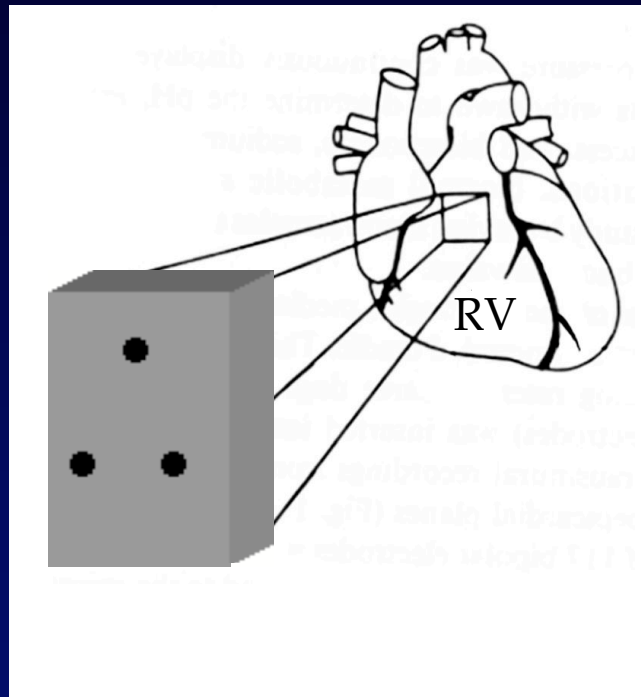


Tensor Diagonalization: Eigenvectors

primary eigenvector:
a proxy for tissue
fiber orientation



Validation in Cardiac DTI

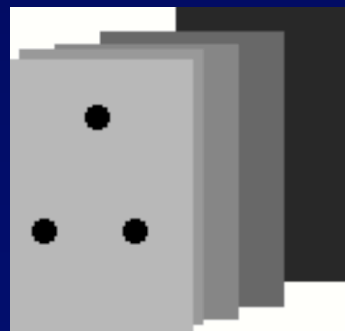


excised right ventricle

MR diffusion tensor imaging
(non-destructive)



fixation

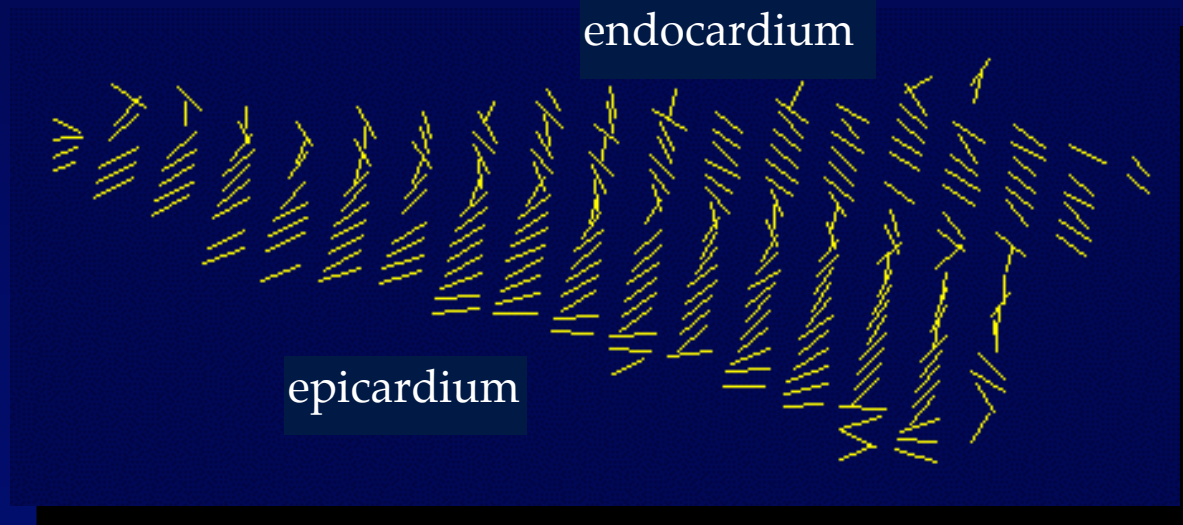


histology

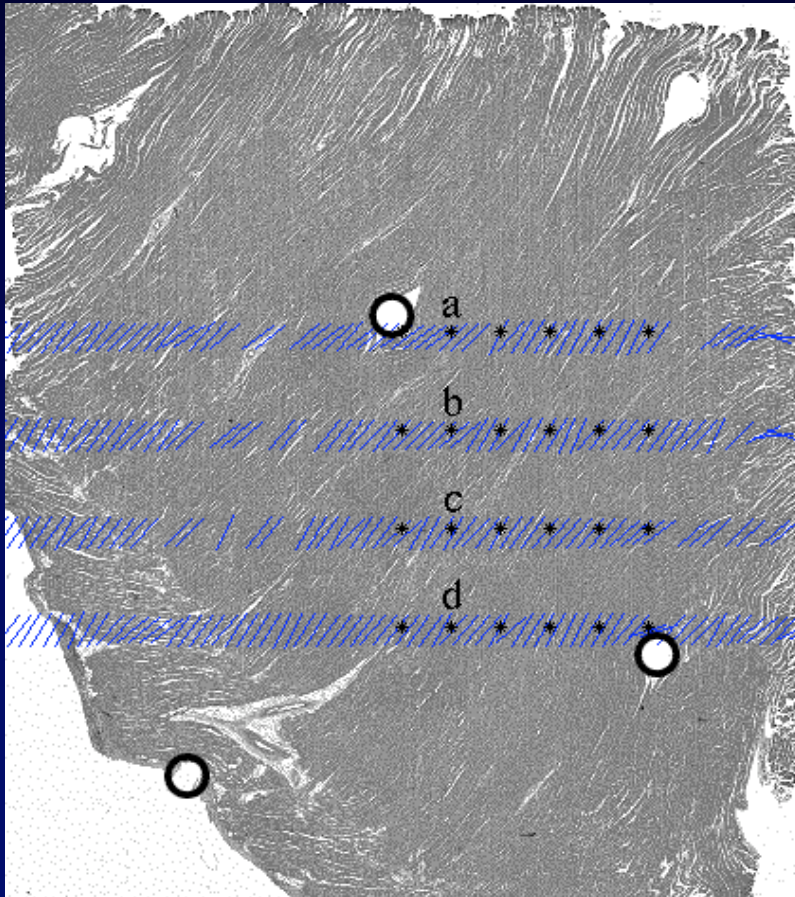
Diffusion Tensor Eigenvector



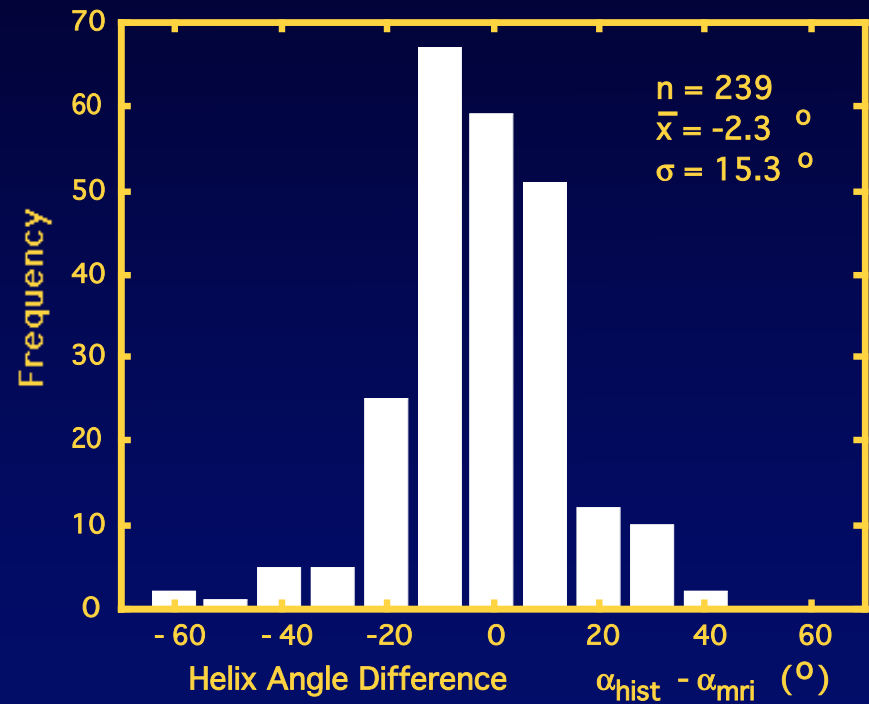
counter-clockwise
transmural fiber rotation



Point-by-Point Comparison

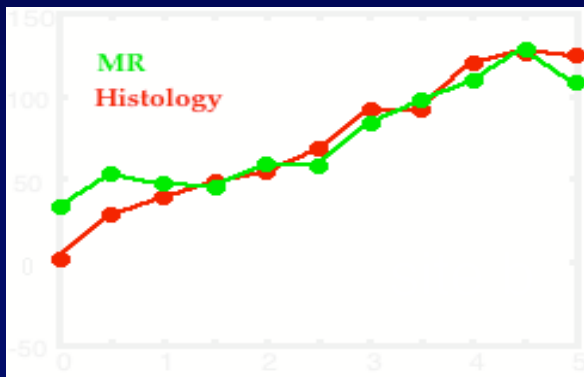


Depth: +2.0 mm

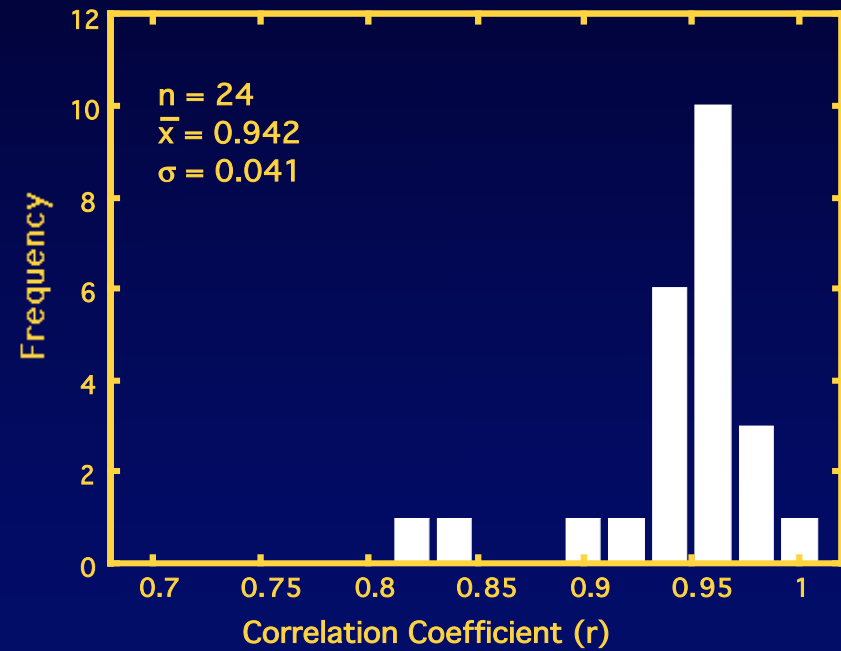


Transmural Fiber Rotation

fiber helix angle (deg)



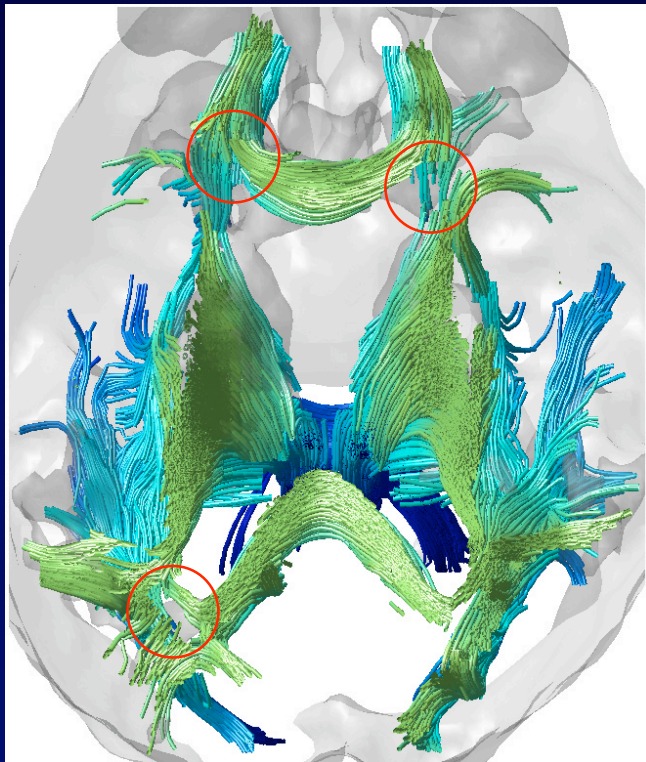
depth from epicardium (mm)



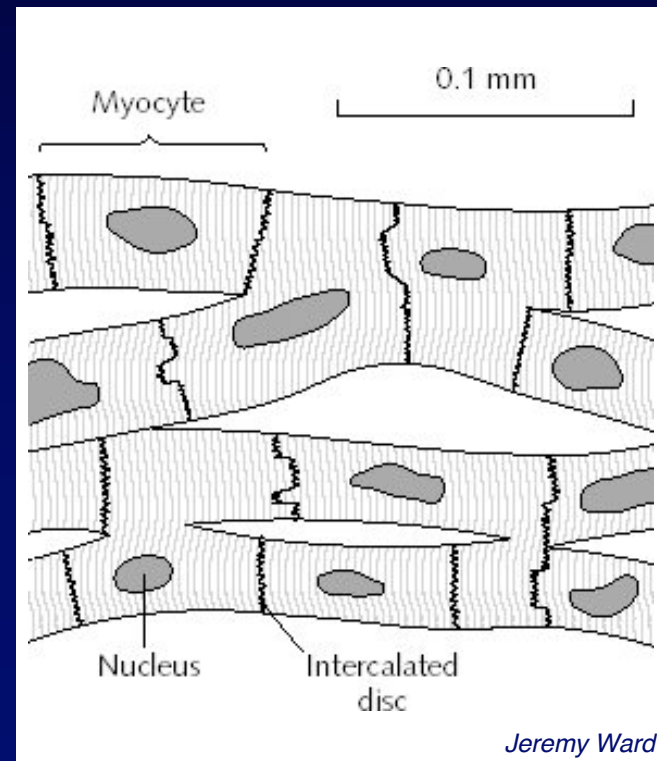
Is DTI Enough?

Assumption: Only One Diffusion Direction

1. Macroscopic merging or crossing fibers



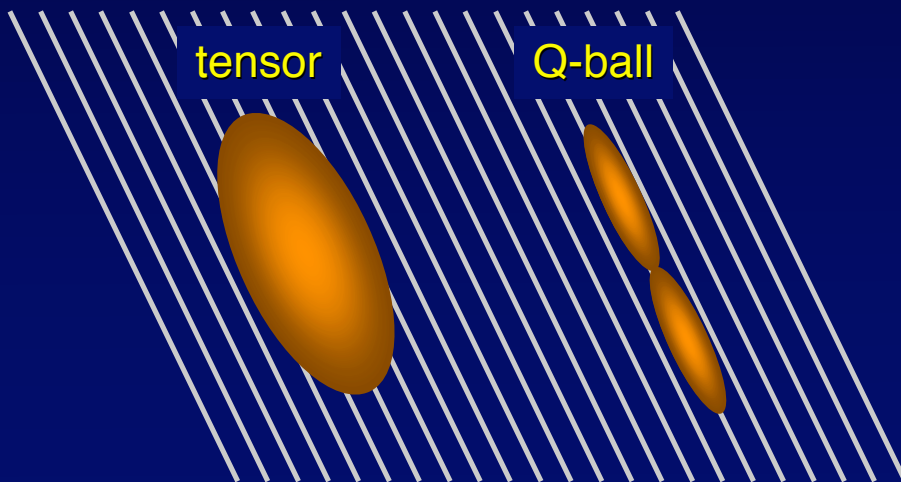
2. Myocyte cellular branching



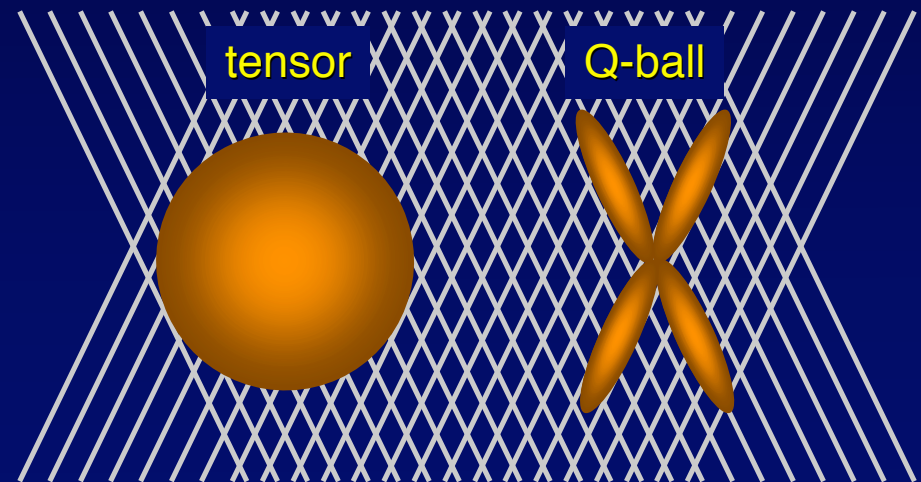
High-Angular Resolution Diffusion Imaging

- More diffusion encoding directions:
- Non-tensor-based diffusion fitting:
“Q-ball”, generalized tensors, etc.

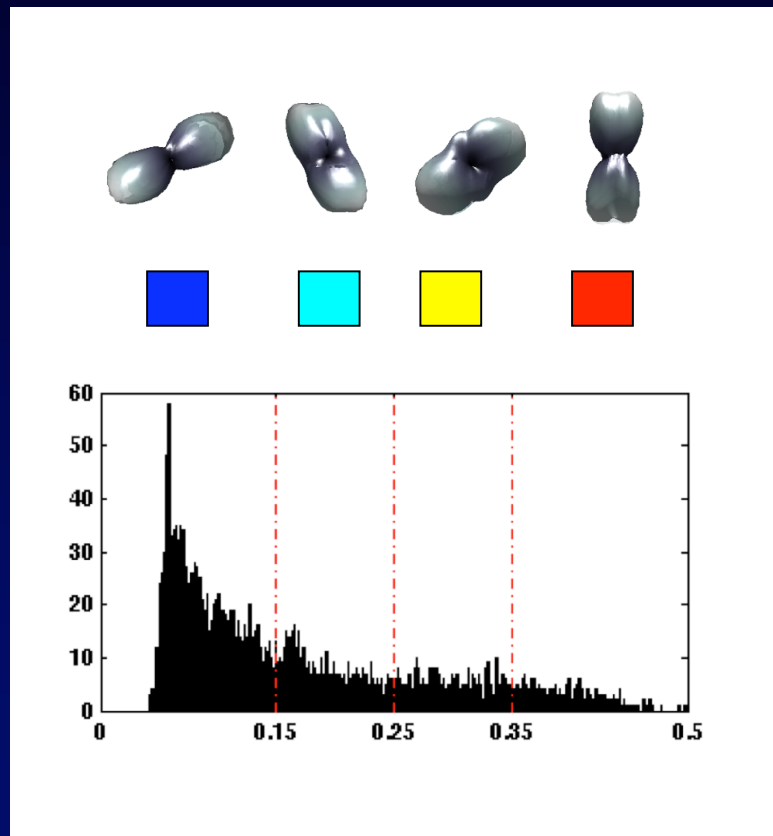
Single fibers



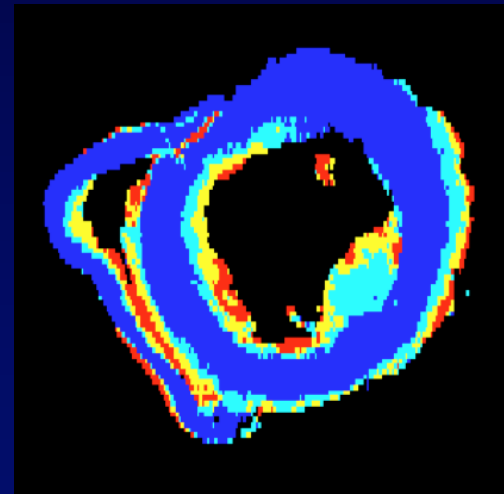
Crossing fibers



Q-ball Imaging of the Myocardium

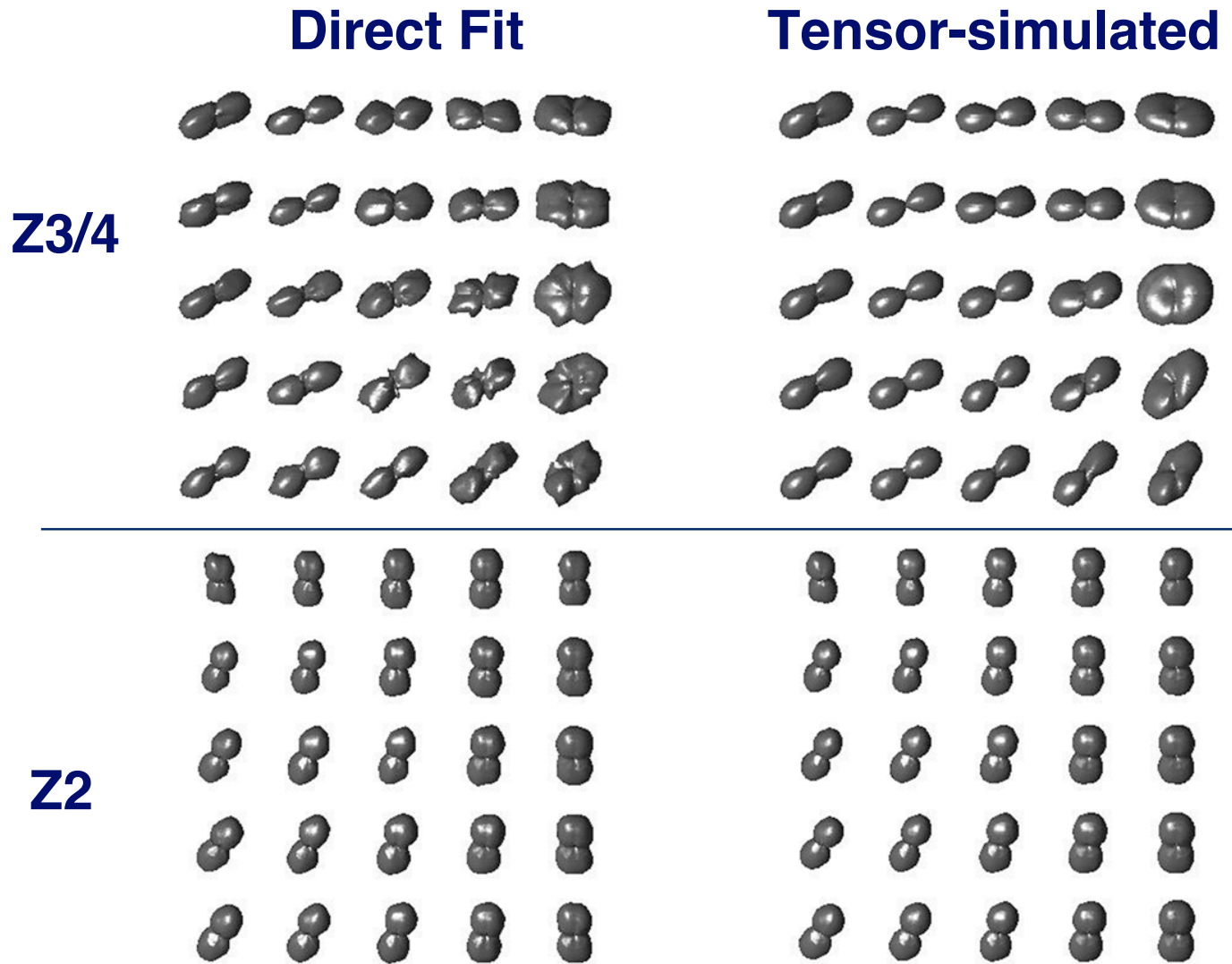
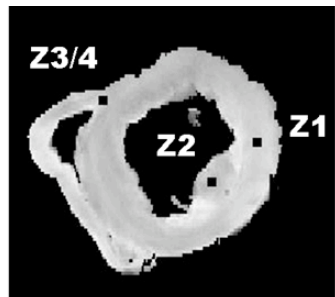


- Fixed canine heart
- Mid ventricular short axis
- 96 directions; $b = 2000 \text{ s/mm}^2$



Shi et al. ISMRM 2007

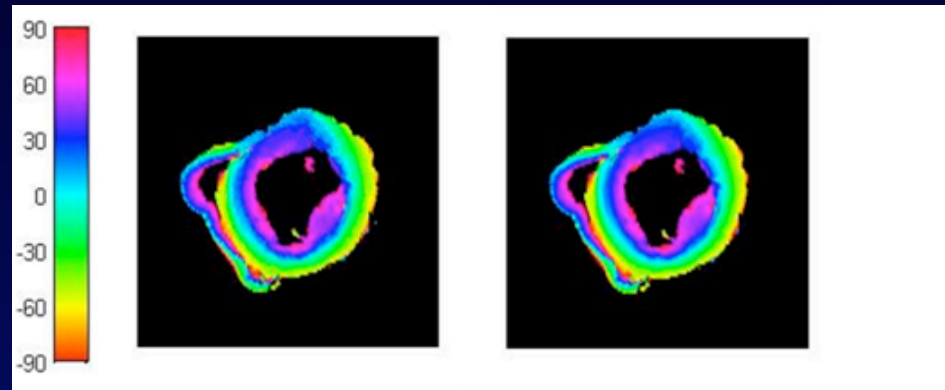
Trouble for DTI?



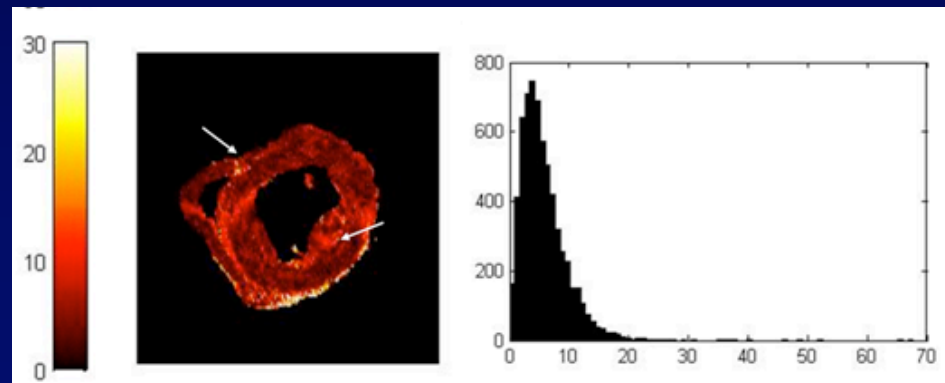
QBI vs DTI

Myocardial Fiber Orientation Mapping

Fiber
Helix Angle



Difference



QBI vs DTI: Implications

1. Small macroscopic differences exist
2. Little impact on fiber orientation mapping
3. Neither can resolve cellular branching

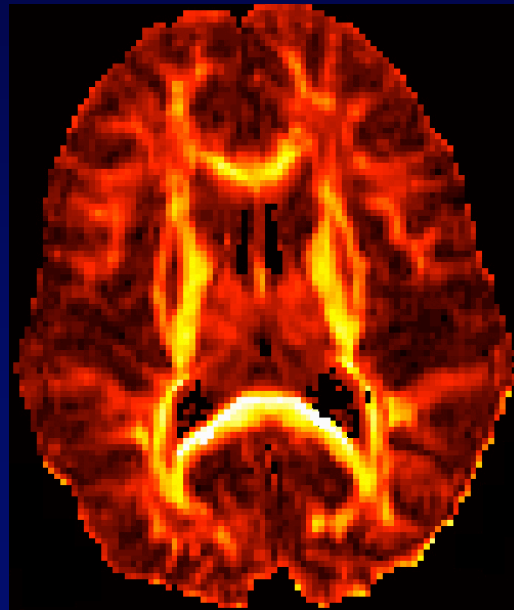
Overview

- Principles and Methods of DTI
- **Engineering Challenges**
- Applications of Cardiac DTI
- Myocardial Structural Models and Atlases

DTI: Engineering Challenges

- diffusion encoding via signal attenuation
- large dataset size -- minimum 7 images
- low spatial & temporal resolution, low quality

128 x 128
single shot DW-EPI
1.0 - 2.0 mm resolution
2.0 mm or larger slice
3D (multislice) scan in
~ 10 min

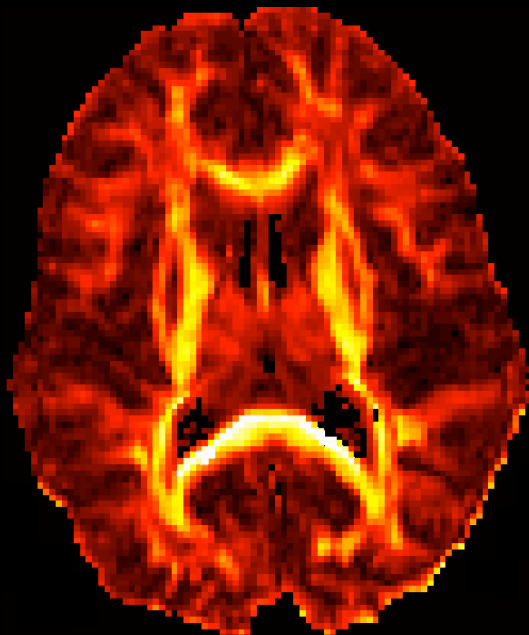


Areas of Development:

- acquisition efficiency
- distortion correction
- data de-noising

Diffusion Tensor “Microscopy”?

human brain
2.0 mm
10 min



mouse brain/heart
100 μm



$$\text{Scan time} \propto \left(\frac{1}{\text{Voxel}}\right)^2$$

1200 YRS!!

Hardware Solutions for SNR

Factor	Change	Real Gain
Stronger magnet	2.3	2
Stronger gradient set	10	3.5
Smaller transceivers	10	10
Longer scans	200	14
Total		1000

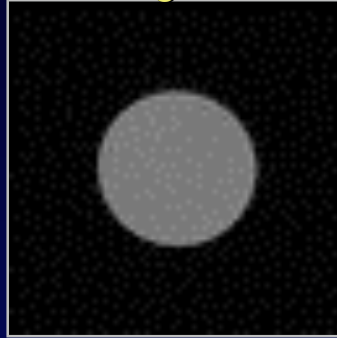
Doable, but not practical

Reducing DTI Scan Time

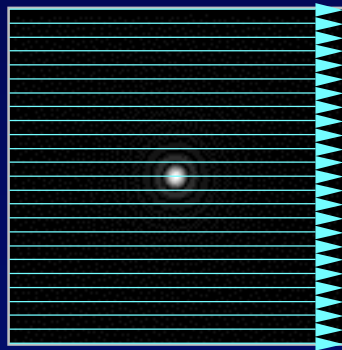
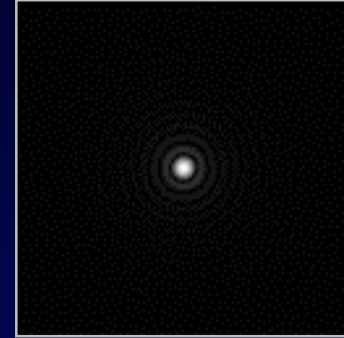
low b



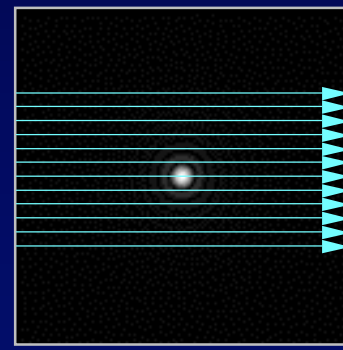
high b



FT of contrast

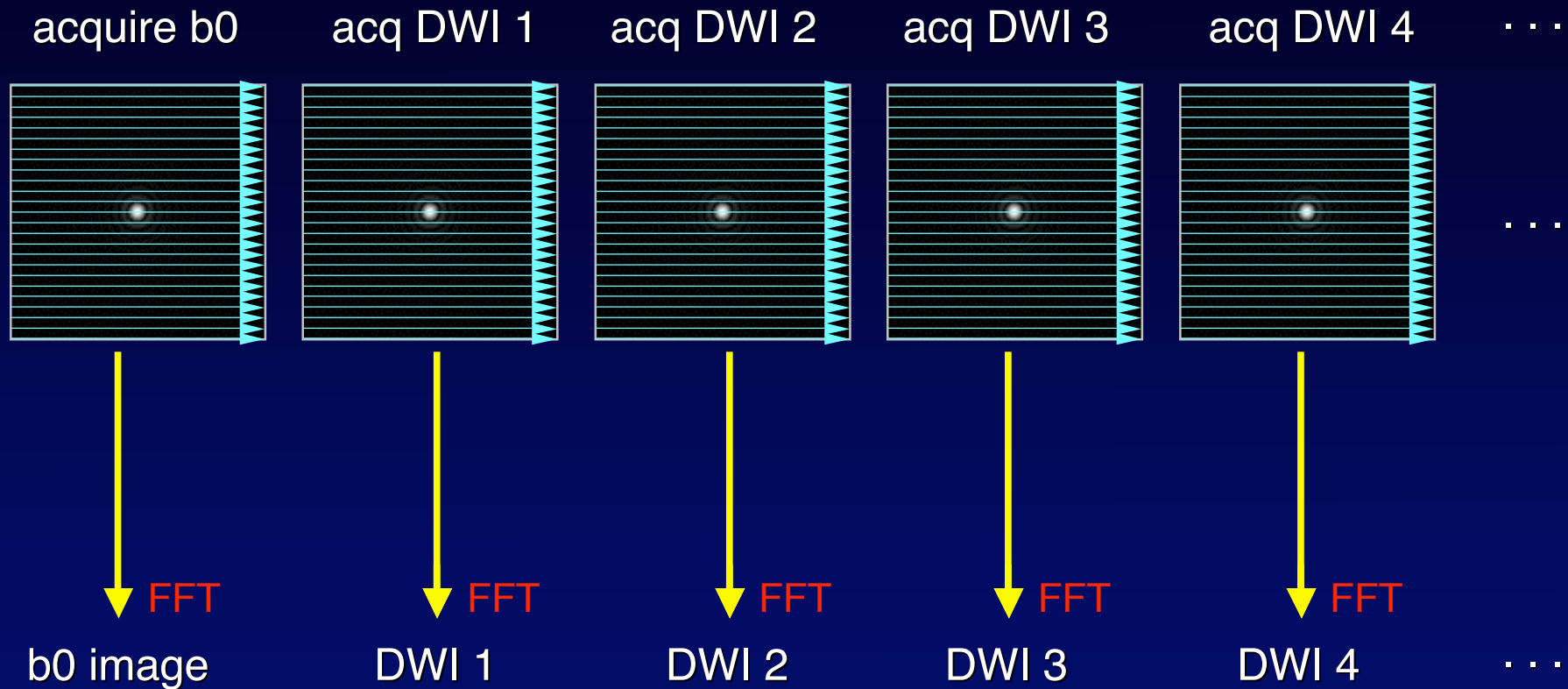


full sampling
(N lines)



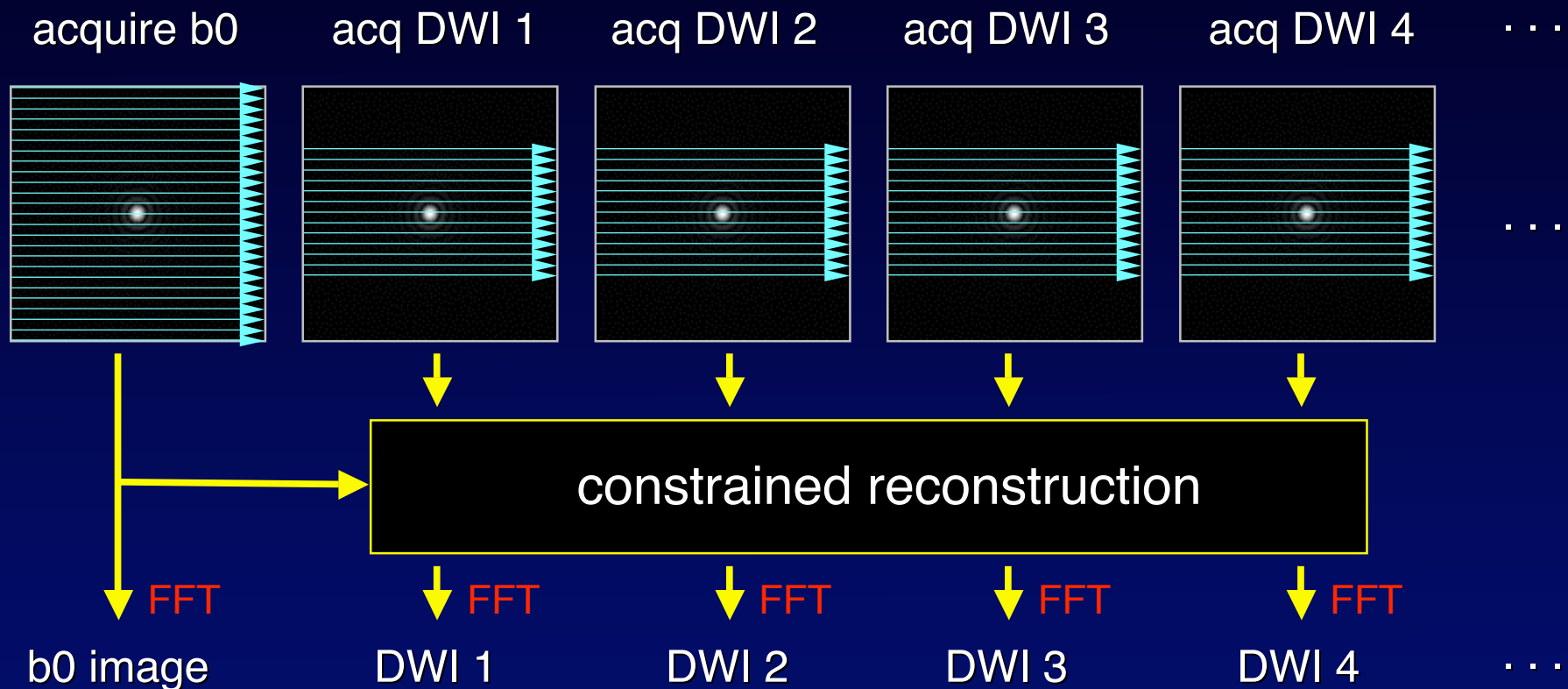
reduced encoding
($N/2$ lines)

Conventional DTI Strategy



Diffusion tensor computation and diagonalization

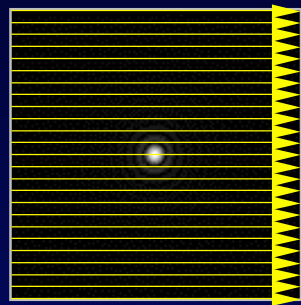
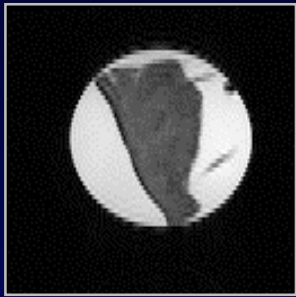
Reduced Encoding DTI Strategy



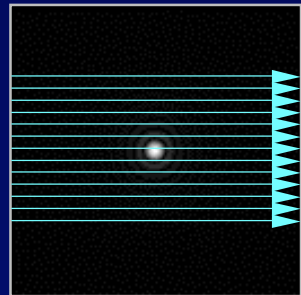
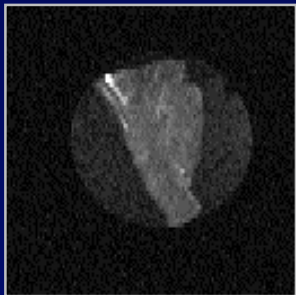
Diffusion tensor computation and diagonalization

Constrained Reconstruction Methods

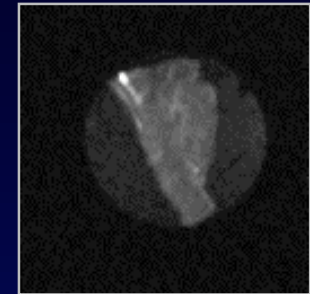
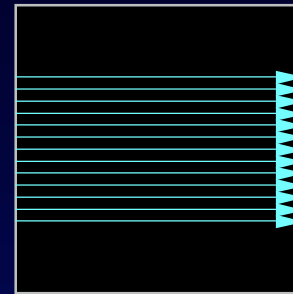
b0



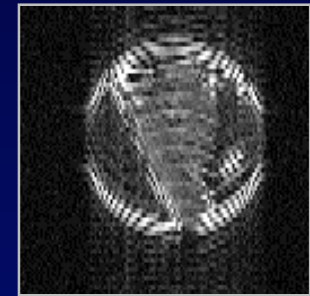
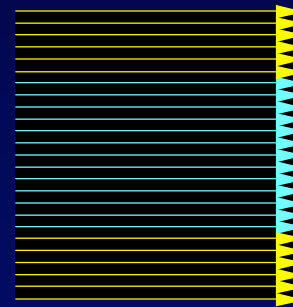
DW



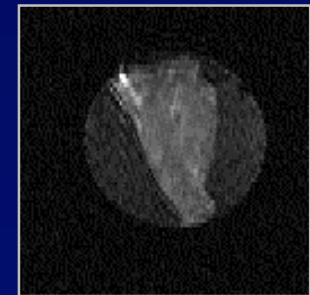
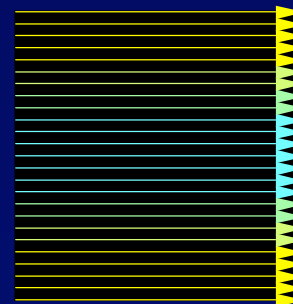
zerofill



keyhole



RIGR



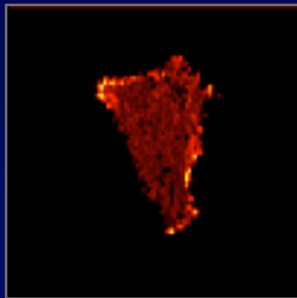
Fiber Orientation Mapping Accuracy

Fiber orientation angle vs “gold standard”

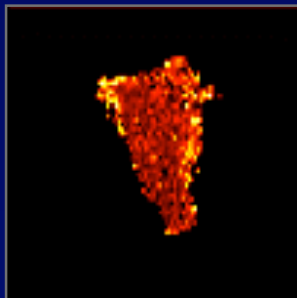
Keyhole[◇]
N @ 50%



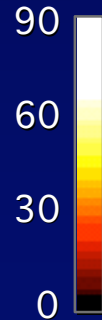
RIGR
N @ 50%



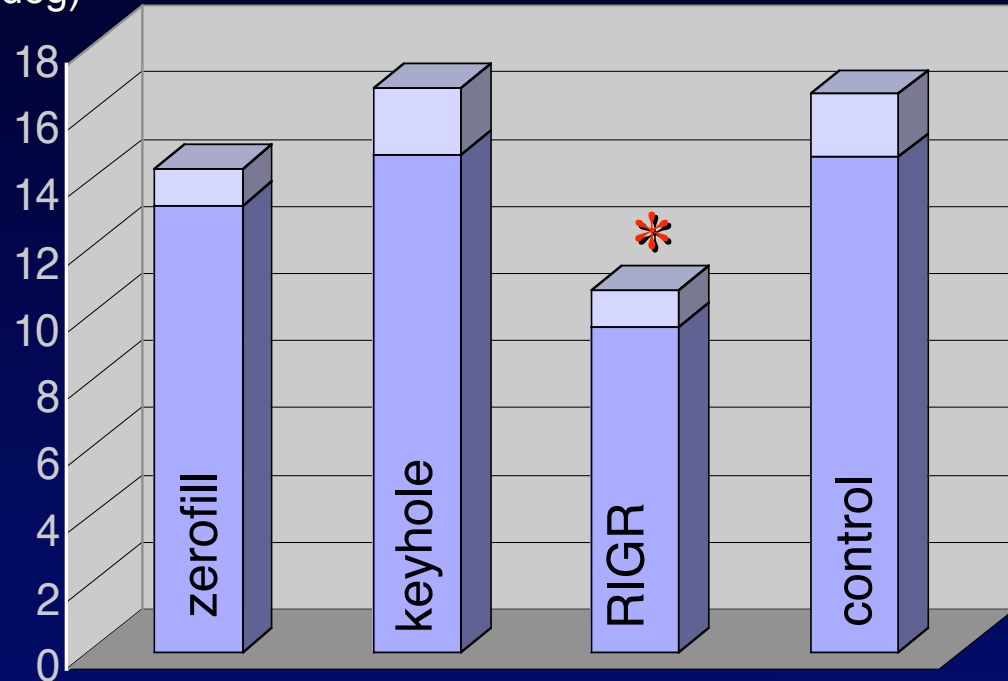
Control
N/2 full



$\Delta\alpha$



(deg)

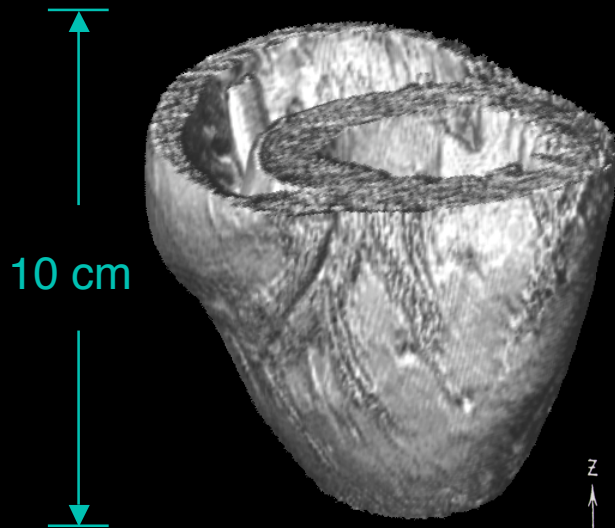


3D DTI: 256 x 128 x 128 matrix size
9 hr vs. 30 hr scan time

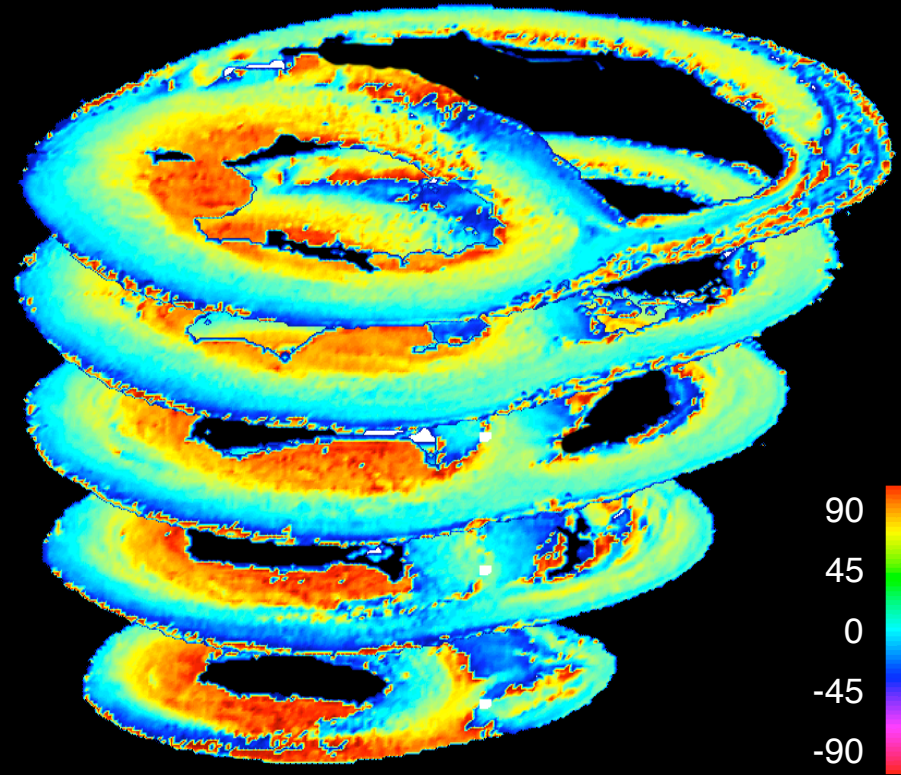
Hsu & Henriquez. J Cardiovasc Magn Reson. 3: 339, 2001

3D Myocardial Fiber Orientation Mapping

dog heart



MR-DTI
selected short-axis slices



fiber helix angle

Streeter et al., 1969

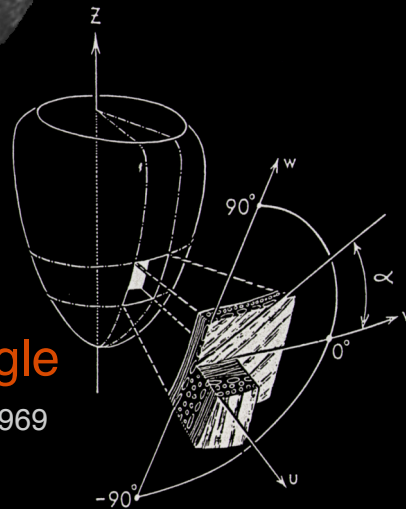
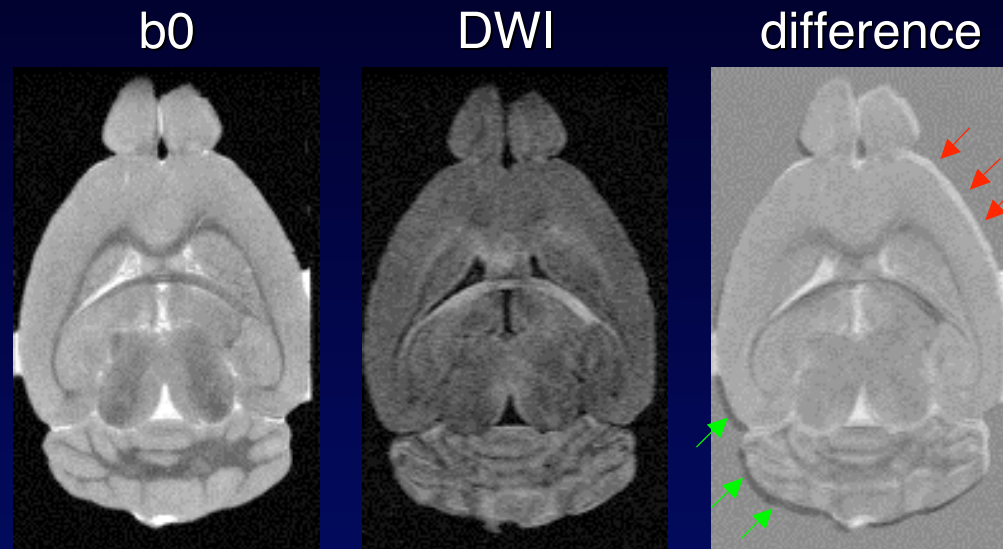


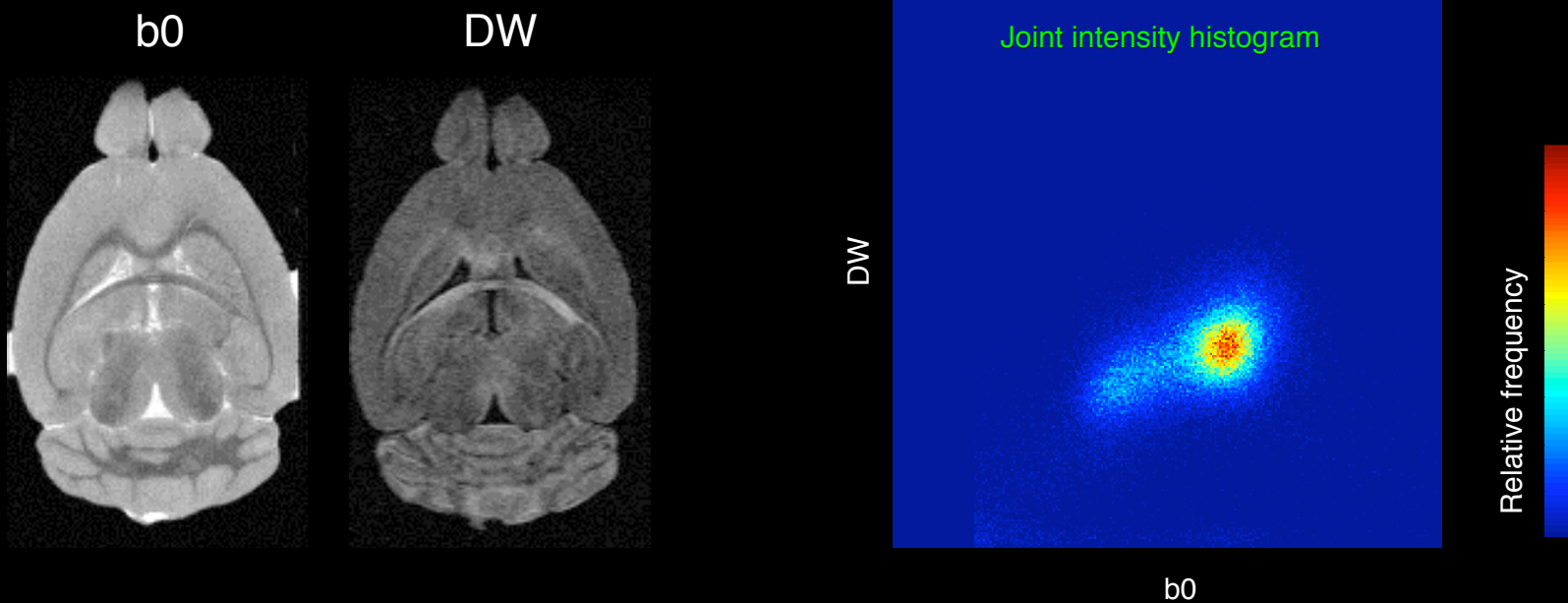
Image Registration



- Diffusion gradient direction dependent
- Causes: eddy-currents, field inhomogeneity, motion, etc
- DT estimation errors at borders
- Loss of fine structures

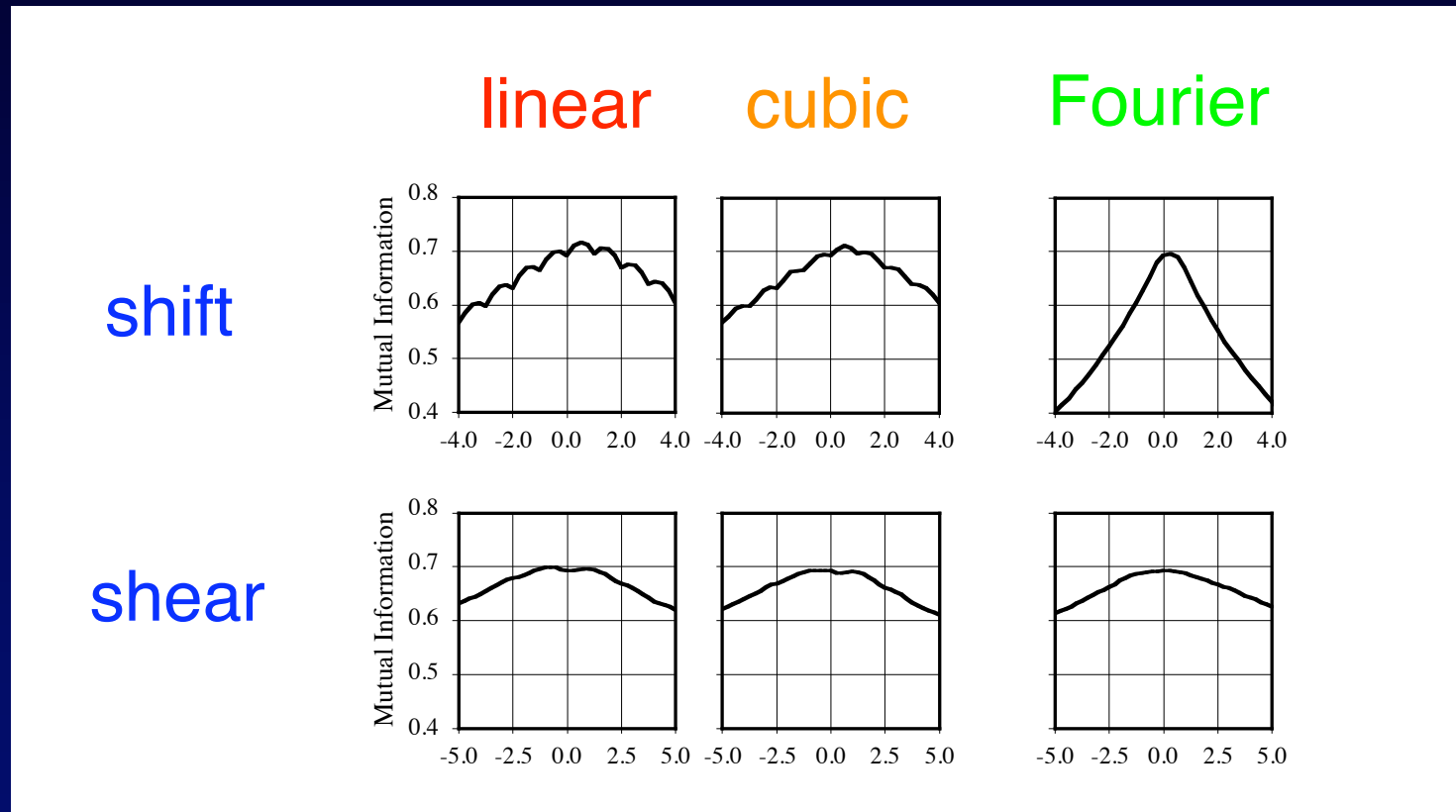
Registration of DW/DT Images

- Challenges:
- 3D landmarks difficult
 - No exact one-to-one intensity correlation



Mutual Information Image Registration

Sub-pixel Interpolation



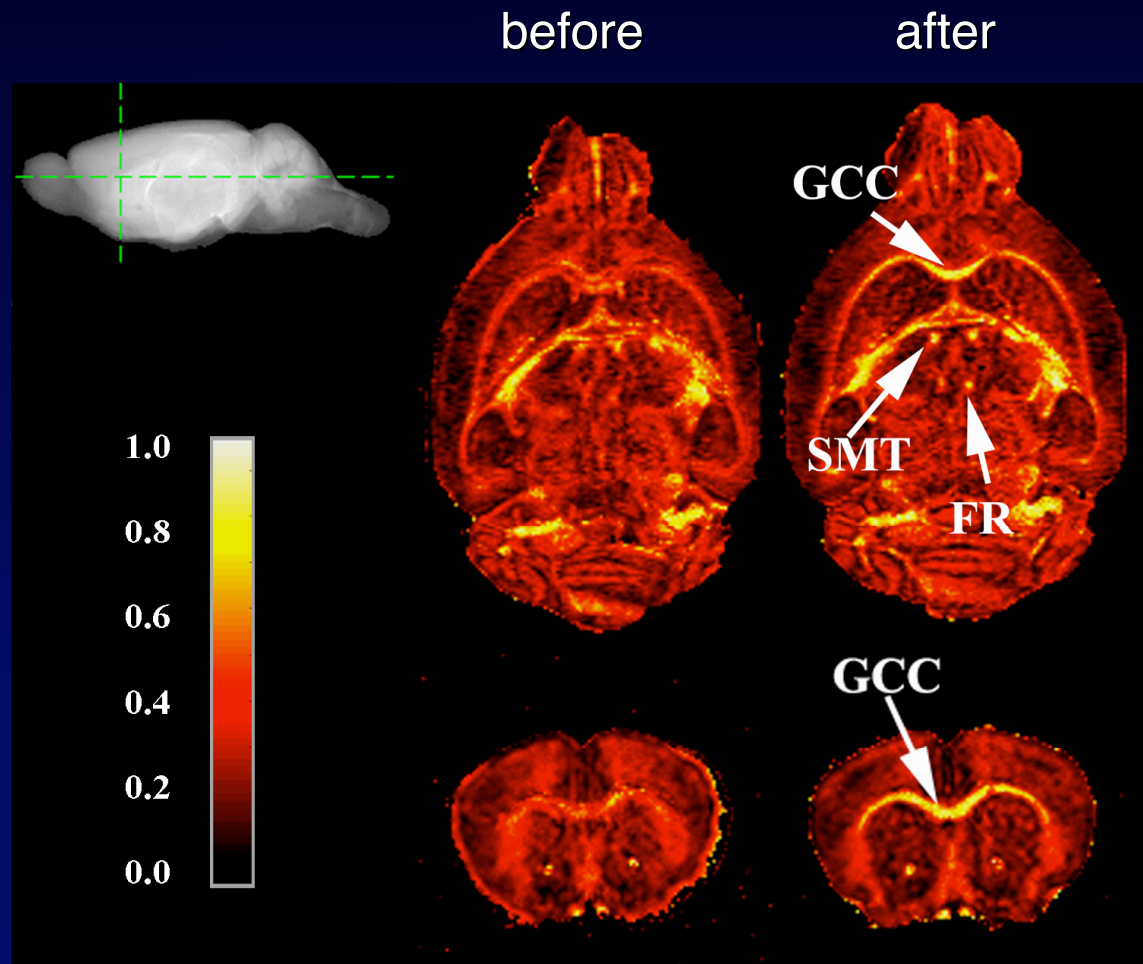
Mistry et al. Magn Reson Med. 56: 310, 2006

Mutual-Information Registration

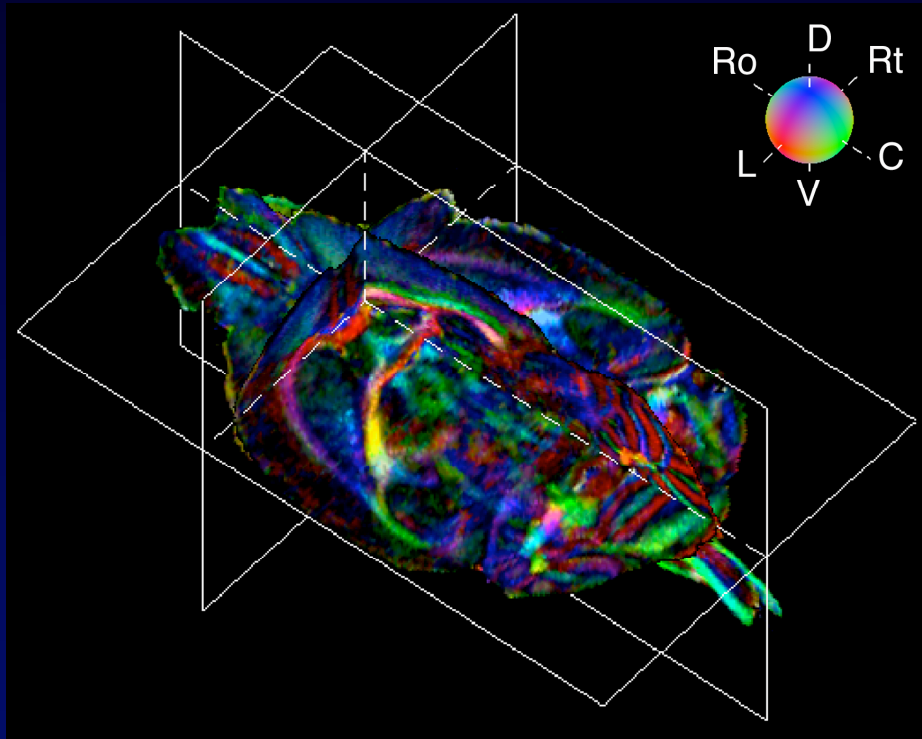
12-dimensional search space:

shift_x*
shift_y*
shift_z*
scaling_x
scaling_y
scaling_z
shear_xy*
shear_yx*
shear_yz*
shear_zy*
shear_xz*
shear_zx*

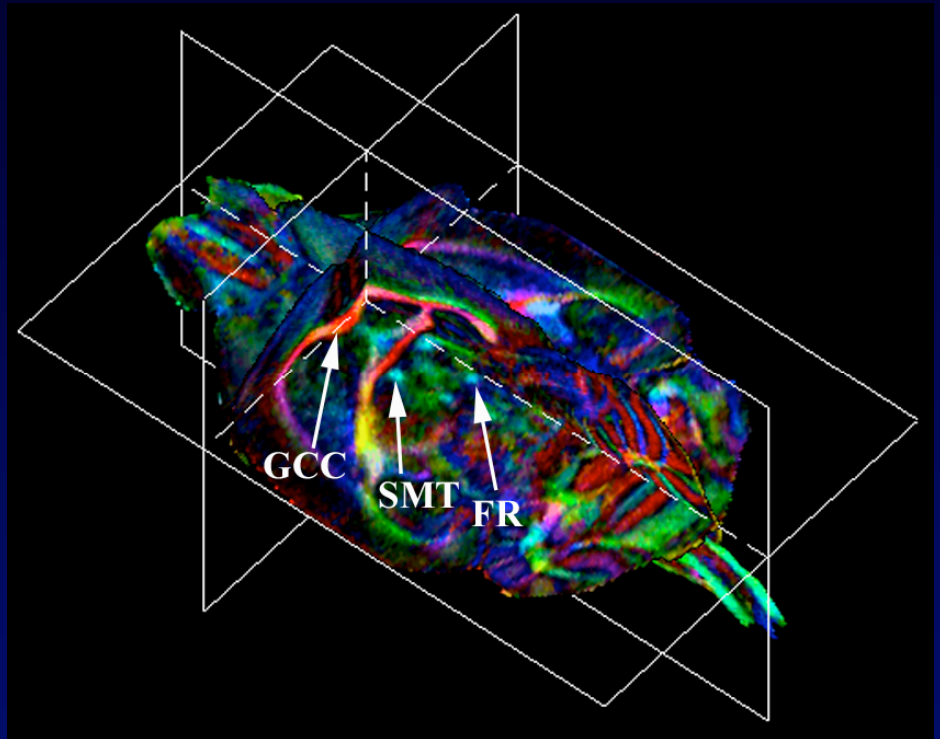
*Fourier deformation



BEFORE



AFTER



Overview

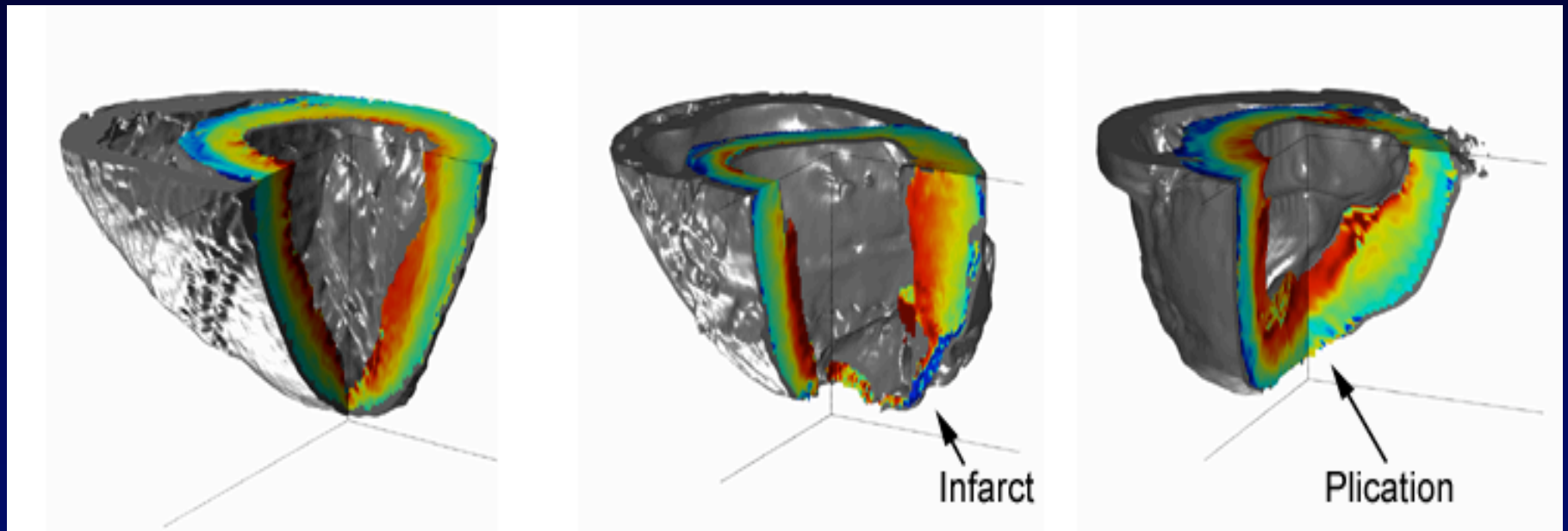
- Principles and Methods of DTI
- Engineering Challenges
- Applications of Cardiac DTI
- Myocardial Structural Models and Atlases

Post-Injury / Surgery Remodeling

Normal

Aneurismal

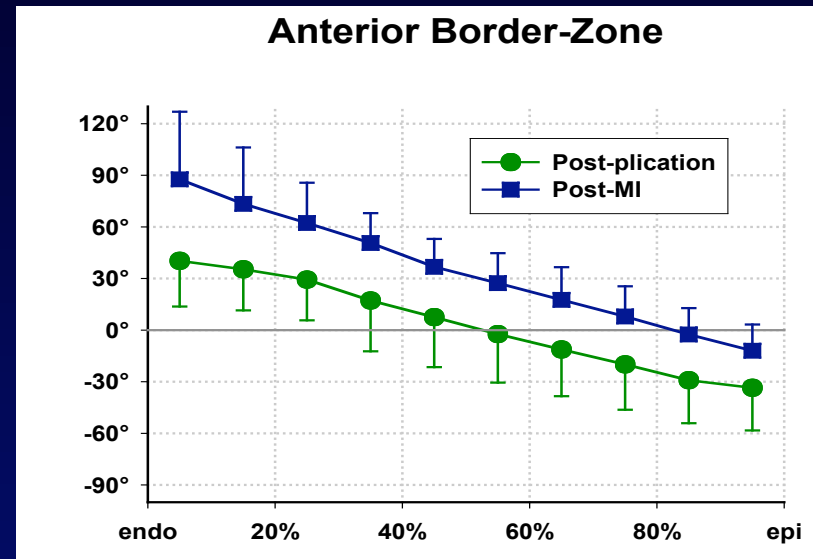
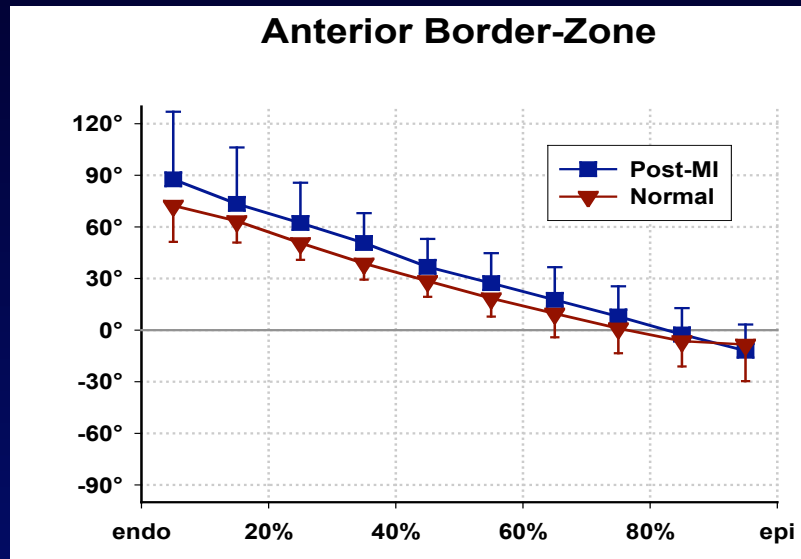
Surgically
Repaired



Sheep hearts
2T, 256 x 128 x 128 acq
10 cm FOV
Scan time: 9.1 hr

Walker et al. J. Thoracic Cardiovasc Surg. 129: 382, 2005

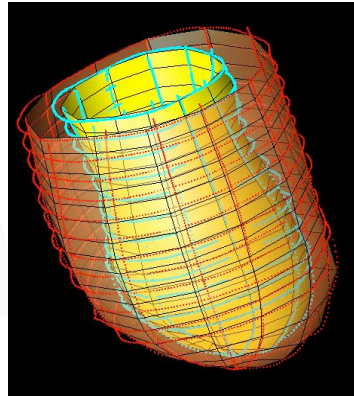
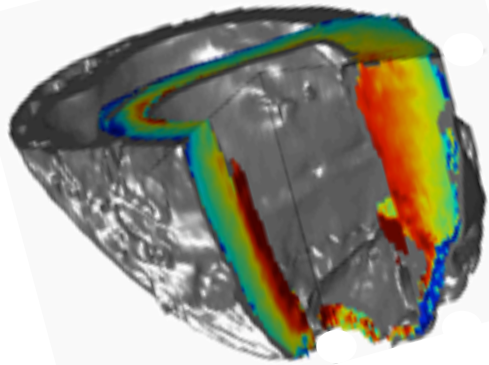
Regional Comparison



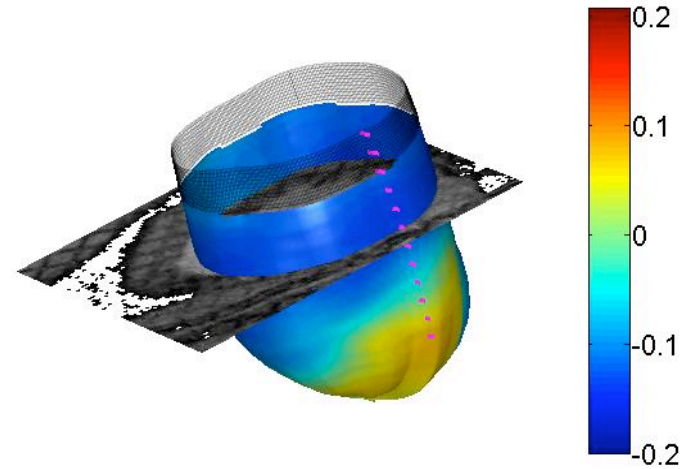
- No change after infarction!!
- Post-plication changes in adjacent regions

Cardiac Mechanics of LV Aneurysm

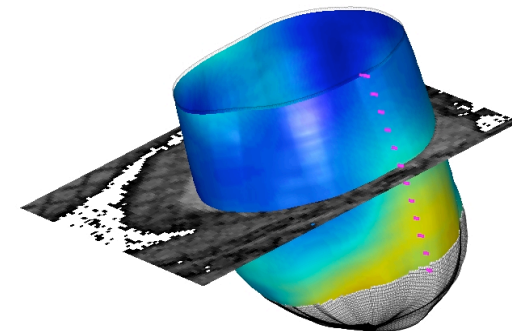
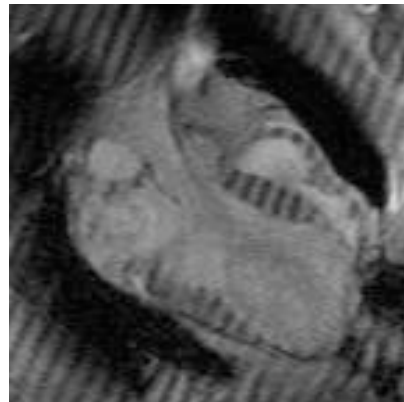
DTI-based FEM



Circumferential Strain



In Vivo Tagging

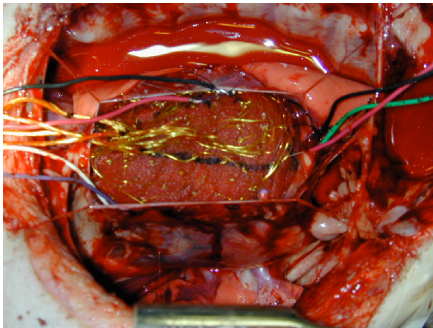
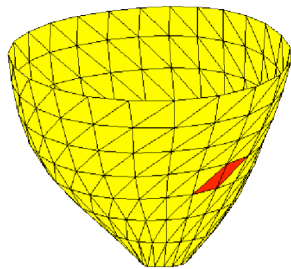


Walker et al. Am J Physiol. 289: H692, 2005

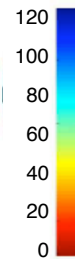
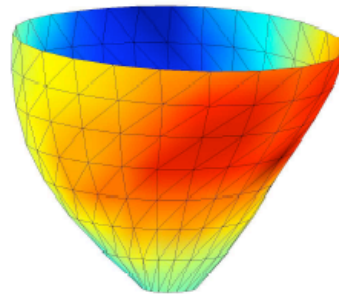
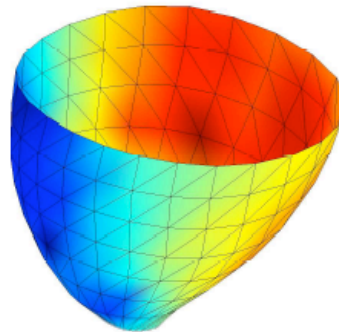
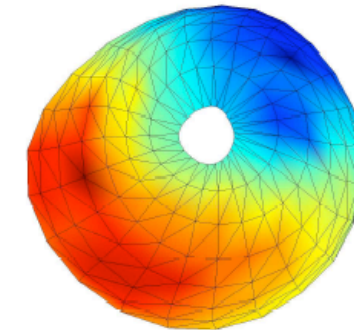
Myocardial Electrophysiology

Canine Ectopic Pacing Action Potential Wave Front

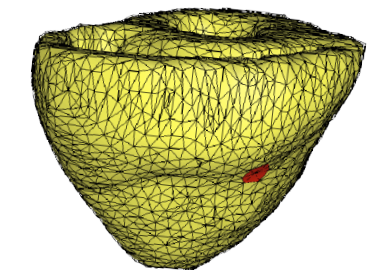
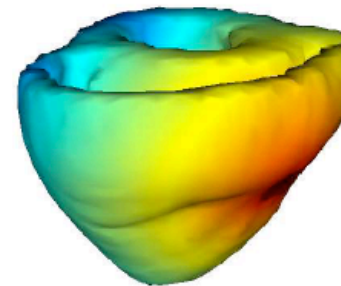
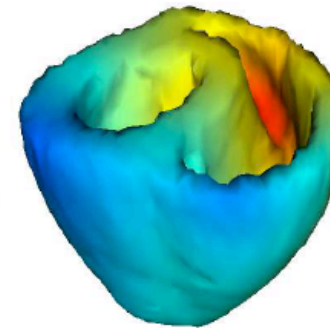
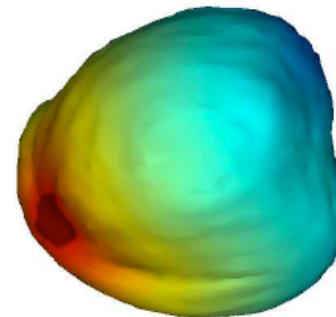
In Vivo Mapping



Courtesy: E. McVeigh (NIH)

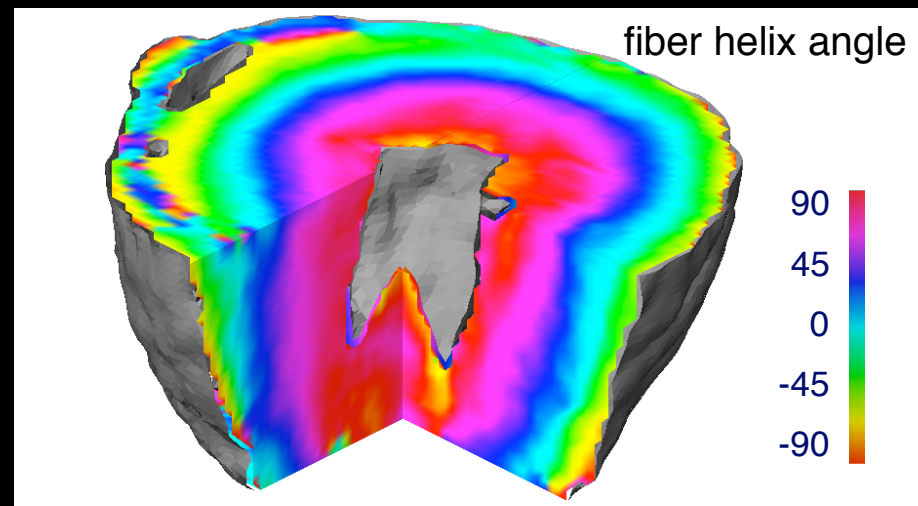
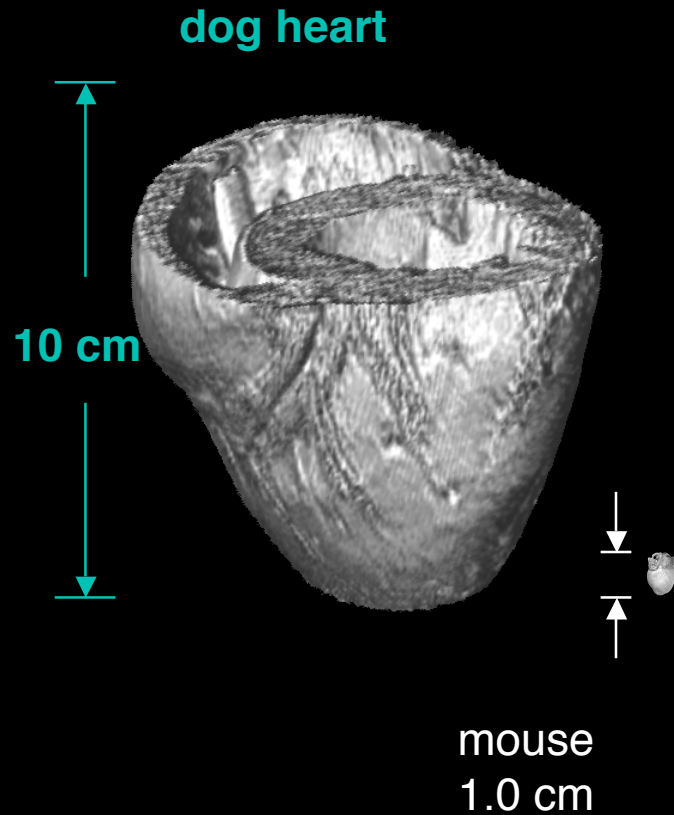


DTI-based FEM



M. Sermesant (INRIA)

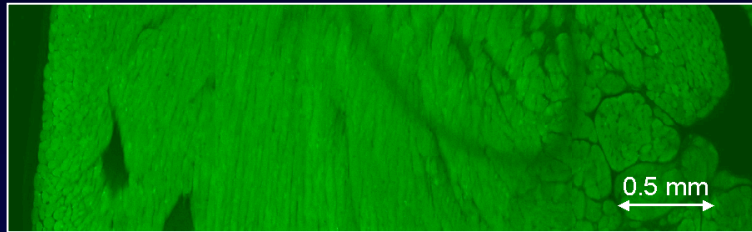
DT Microscopy of Mouse Hearts



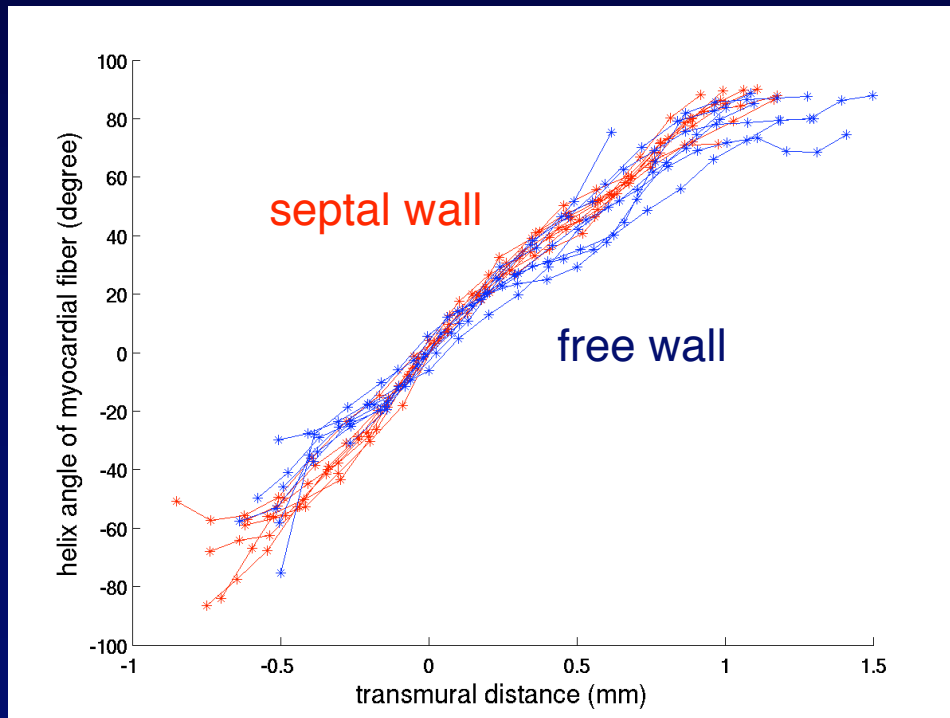
9T, 100 μm isotropic resolution
200,000+ measurement points

Jiang et al. Magn Reson Med. 52: 4453, 2004

LV Transmural Fiber Helix Angles



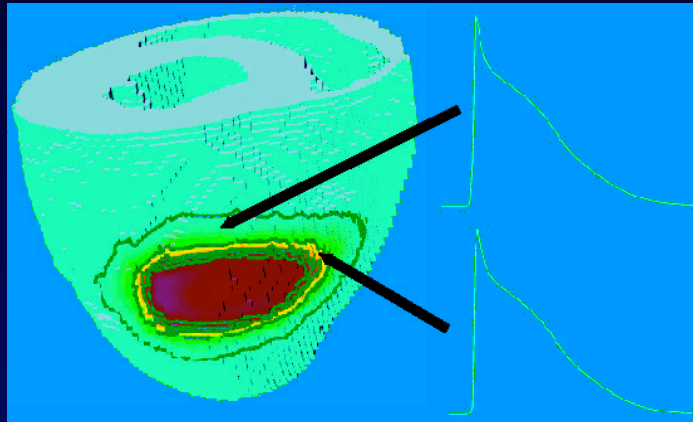
Courtesy: K. Pandya (UNC-CH)



Fiber Angle Mapping
Accuracy: $\pm 5^\circ$

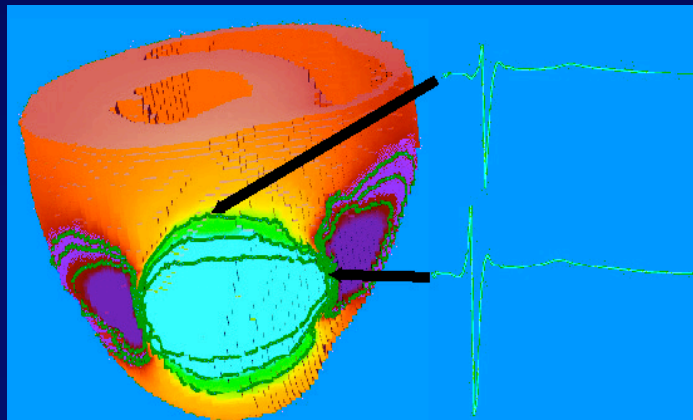
Mouse Heart Electrophysiology

transmembrane
potential
5 ms post pacing



Collaborators:
J. Tranquillo (Duke)
C. Henriquez
D. Weinstein (Utah)
G. Kindleman

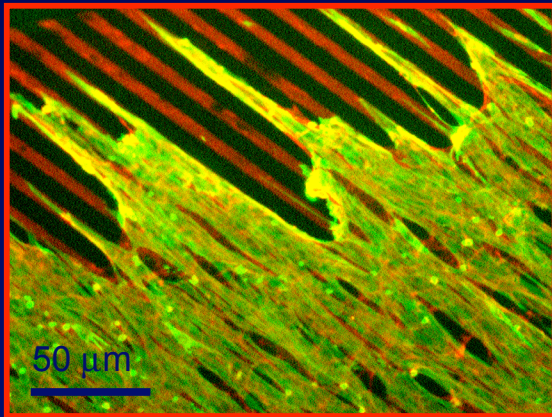
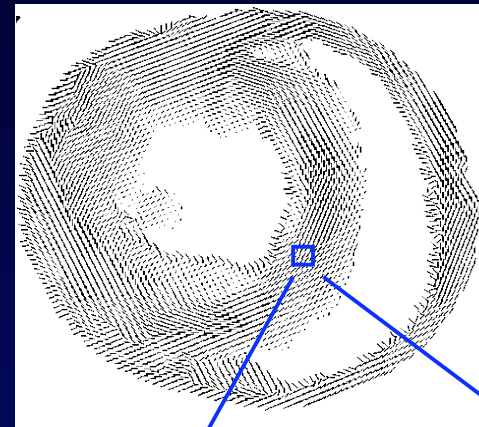
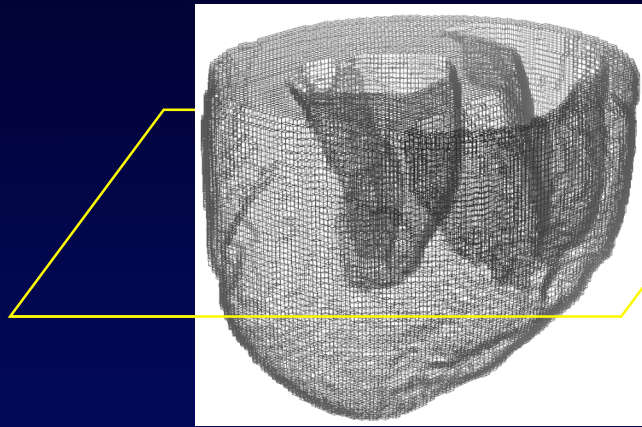
extracellular
potential
5 ms post pacing



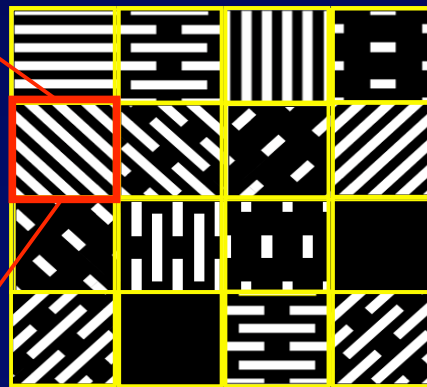
DTI and Tissue Engineering

“Biologically Inspired” 2D Heart Slice

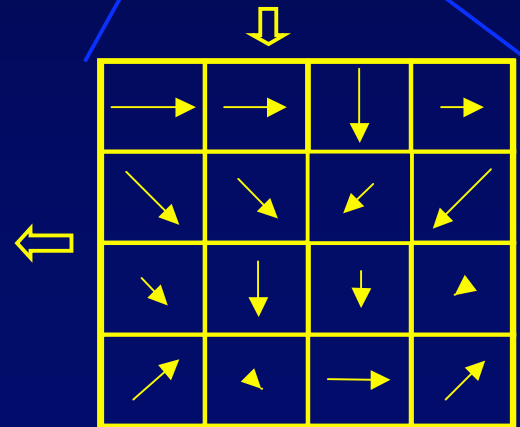
N. Bursac (Duke)



myocyte culture



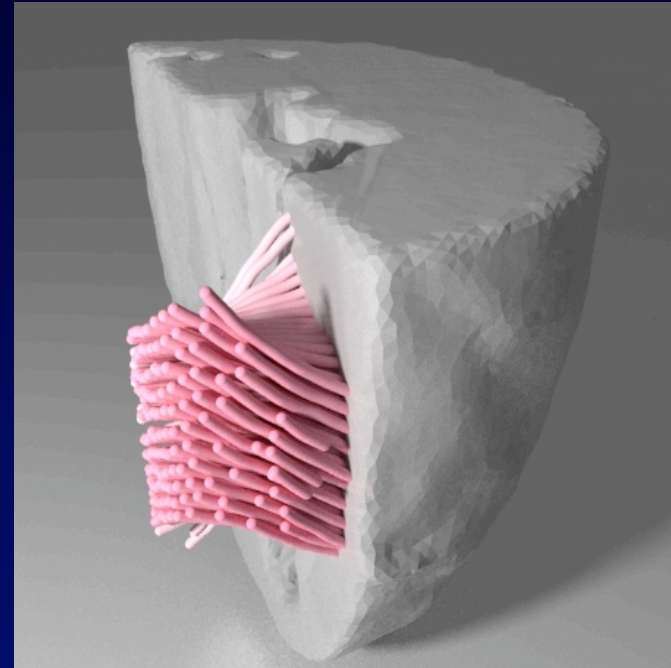
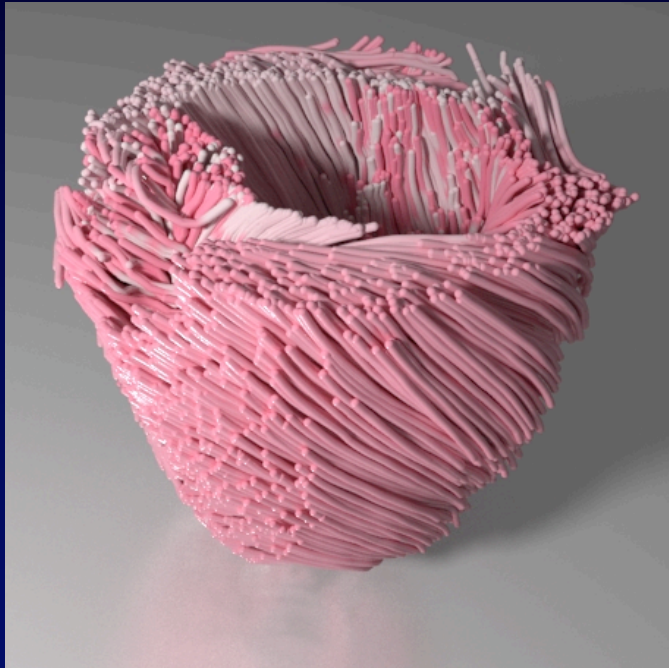
fibronectin etch



fiber direction vectors

Myocardial Fiber Visualization

DTI-based renderings of a rat LV



G. Gullberg, LBNL

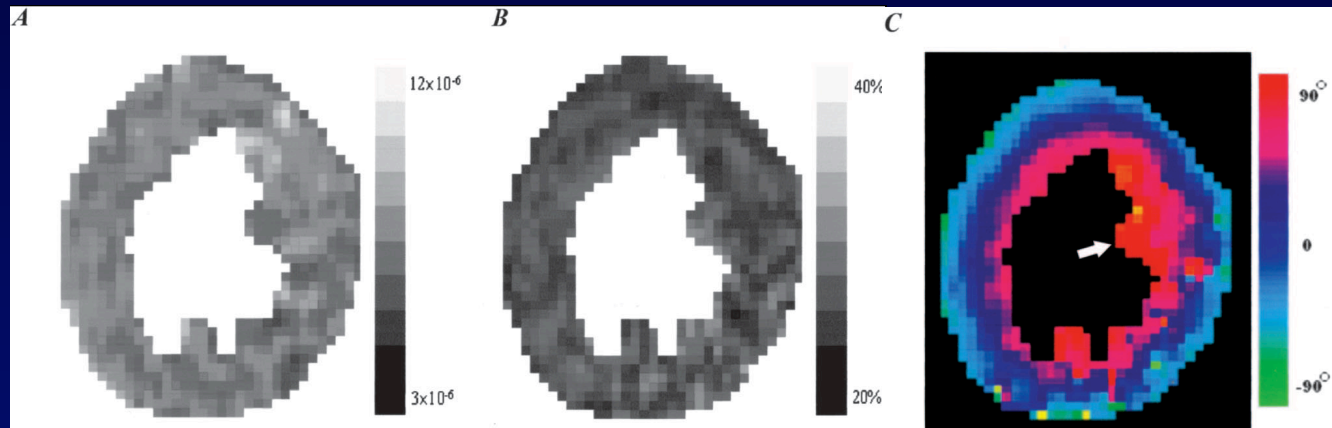
In Vivo Cardiac DTI?

Possible, but . . .

MD

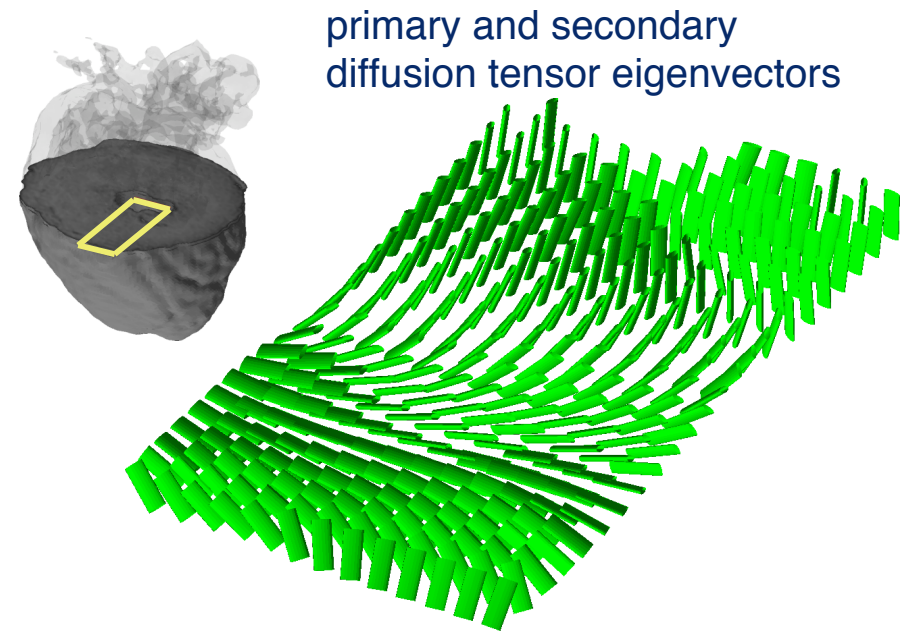
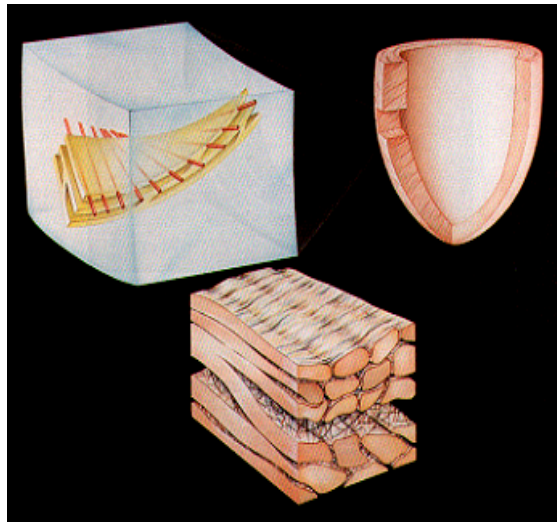
FA

α_H



Wu et al. Circulation. 114: 1036, 2006

Myocardial Sheet Structure



- Morphologically consistent
- Not fixation artifact
- Biophysical origin still unknown

Overview

- Principles and Methods of DTI
- Engineering Challenges
- Applications of Cardiac DTI
- Myocardial Structural Models and Atlases

Myocardial Structural Models /Atlases

Key Challenges

1. Fiber Orientation Measurement:

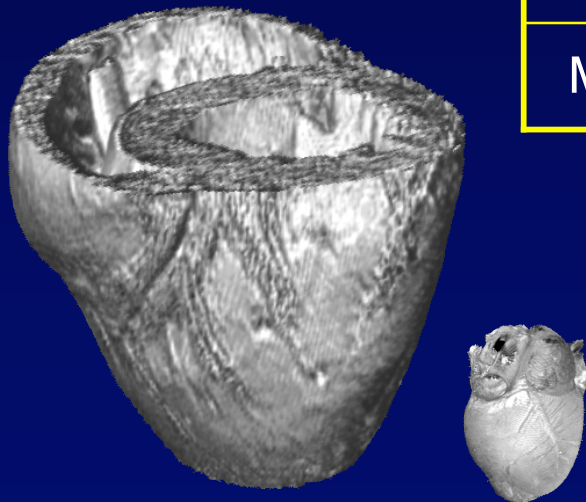
- alternative to histology
- suitable for the mouse

2. Statistics:

- inter-species variability
- intra-species variability
- atlas?

Myocardial Fiber Orientation: Inter-Species Variability

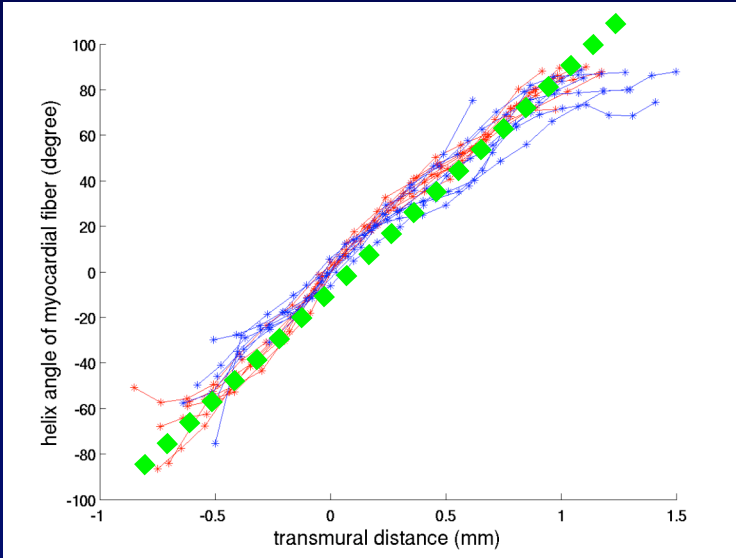
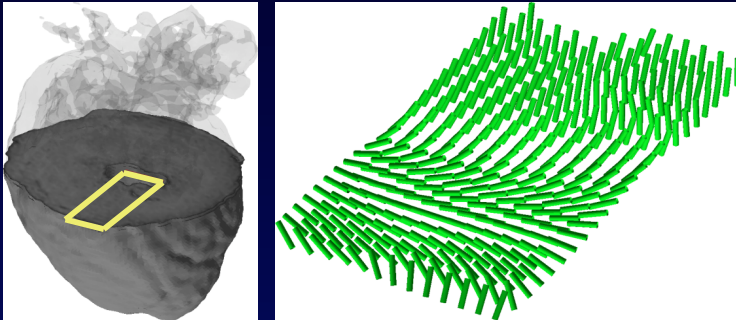
Species	N	Scanner	FOV	SNR
Sheep	5	2.0 T	10 cm	125
Rabbit	6	7.0 T	4.0 cm	102
Mouse	10	9.4 T	1.2 cm	95



3D DTI:

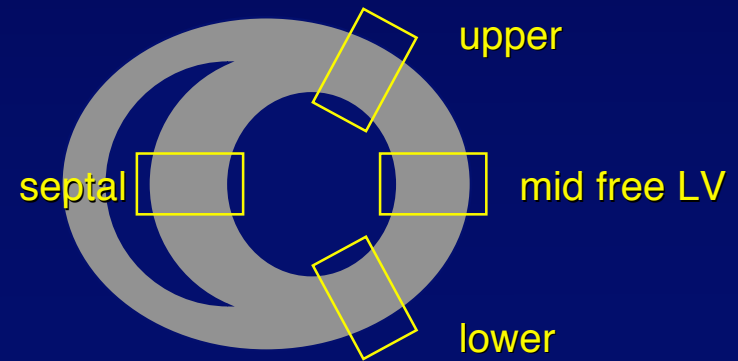
- normal, fixed in end-systole
- 128 x 128 x 128 matrix
- b0 + DWI in 12 optimized directions
- 9.1 hr acquisition

Myocardial Fiber Orientation: Inter-Species Variability



- subepicardial helix angle
- epi-to-endocardial range
- linearity

2-way ANOVA comparing
across species and
myocardial zones



	Species	Septal	Mid Free wall	Upper Free wall	Lower Free wall
Range	Mouse	69.0 ± 17.8	68.9 ± 17.4	75.3 ± 17.1	72.4 ± 22.4
	Rabbit	44.0 ± 11.3	48.9 ± 10.5	47.6 ± 11.7	39.4 ± 9.70
	Sheep	38.0 ± 9.92	54.5 ± 7.27	54.4 ± 10.8	51.7 ± 10.7
Subepicardial Helix Angle	Mouse	-58.6 ± 9.53	-50.2 ± 14.7	-35.9 ± 14.6	-46.9 ± 14.4
	Rabbit	-42.6 ± 14.9	-29.9 ± 14.6	-27.7 ± 11.4	-23.7 ± 13.9
	Sheep	-28.2 ± 19.2	-30.2 ± 8.74	-24.3 ± 9.64	-26.6 ± 9.26
Linearity	Mouse	0.98 ± 0.011	0.99 ± 0.011	0.97 ± 0.025	0.98 ± 0.017
	Rabbit	0.93 ± 0.14	0.94 ± 0.038	0.94 ± 0.050	0.97 ± 0.028
	Sheep	0.91 ± 0.070	0.95 ± 0.044	0.95 ± 0.055	0.94 ± 0.052

No significant zonal difference detected,
but species-species differences are significant

	Range	Sub-epi α_H	Linearity
mouse-sheep	YES	YES	YES
mouse-rabbit	YES	YES	YES
rabbit-sheep	YES	YES	NO

Inter-Species Variability: Implications

1. Biomechanics:

- fewer myocyte in smaller hearts
- steeper transmural angle = higher torsion?

2. Myocardial modeling:

- cannot scale across species
- at least hearts of different sizes

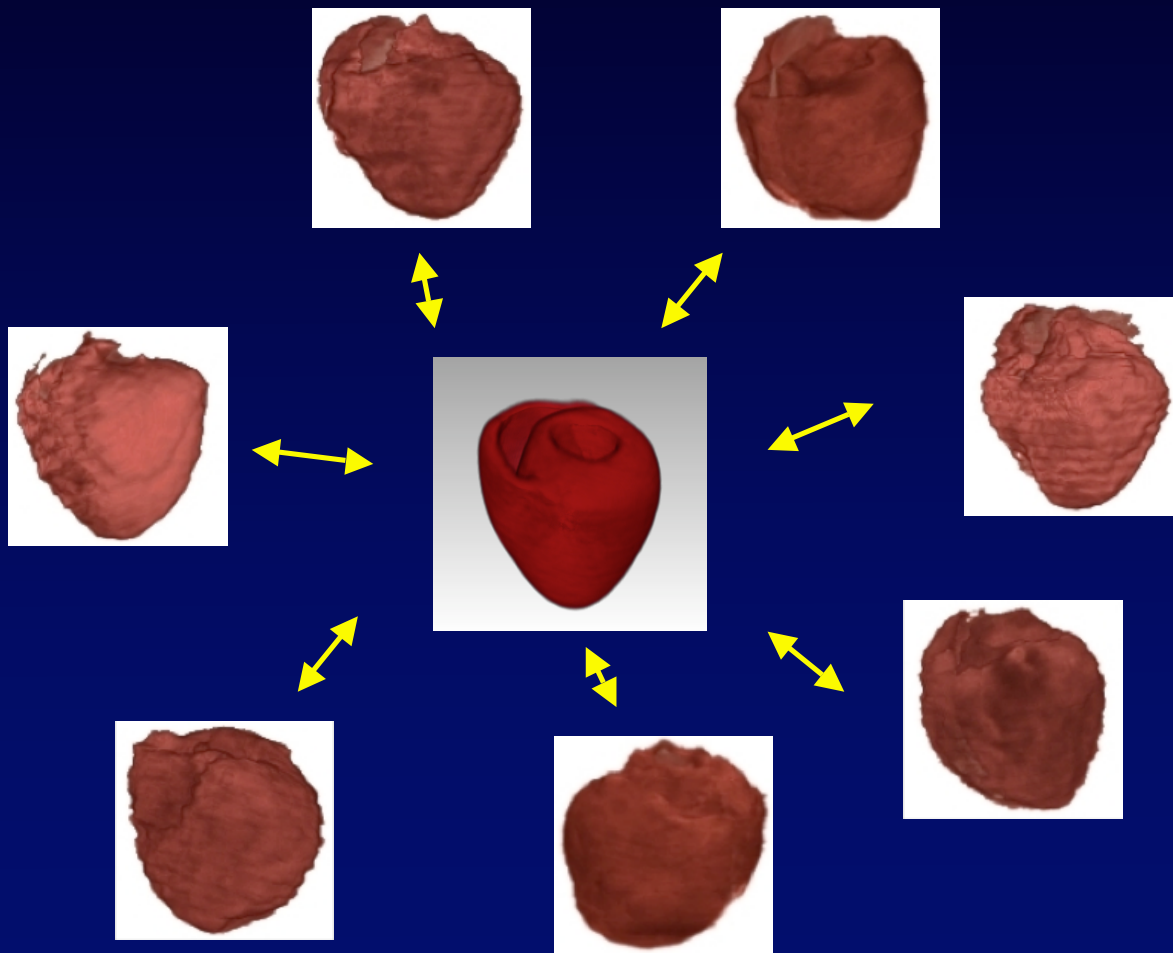
Myocardial Fiber Orientation: Intra-Species Variability



Areas of Development:

- define anatomically-equivalent points
- quantitative comparison of tensor fields

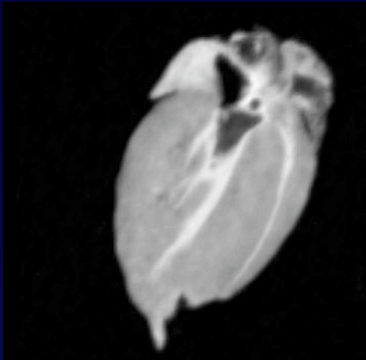
Large Deformation Diffeomorphic Metric Mapping (LDDMM)



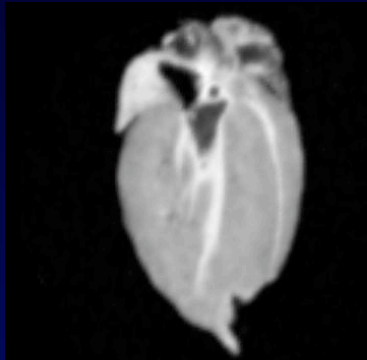
- infinite DOF
- invertible

Image Processing Pipeline

original



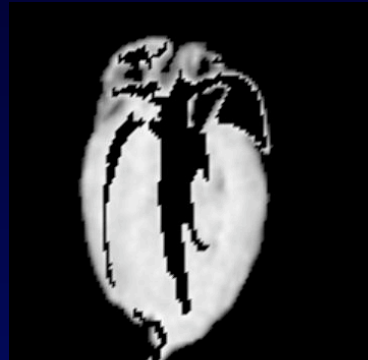
align



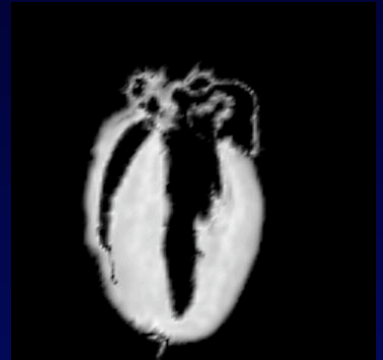
segment



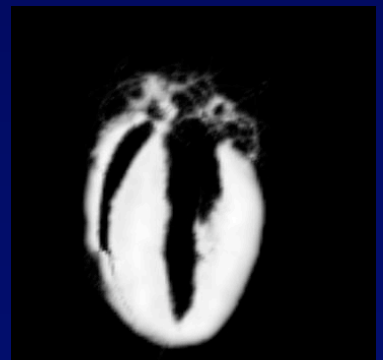
affine



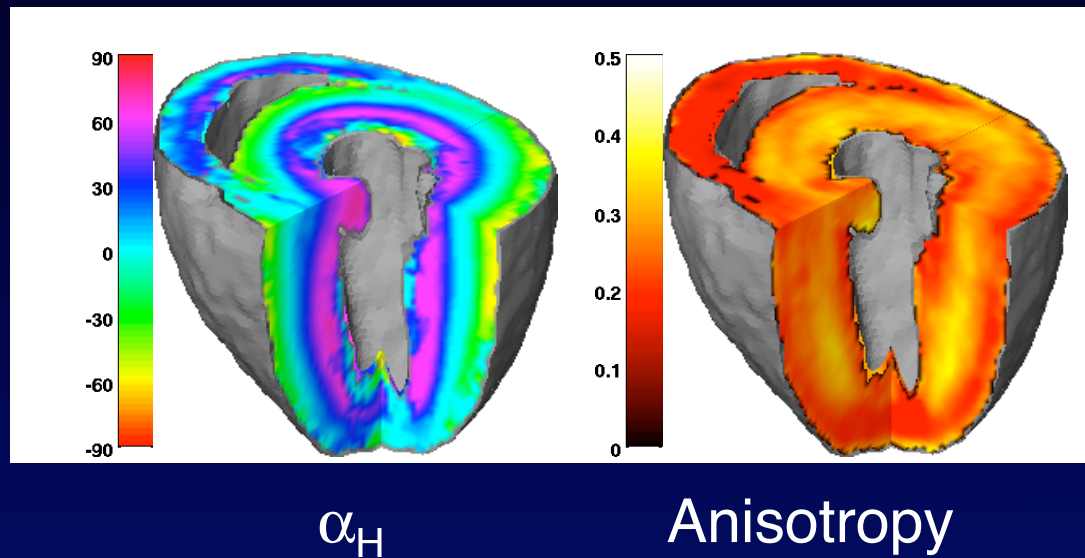
LDDMM



atlas



Statistics of Group Averages



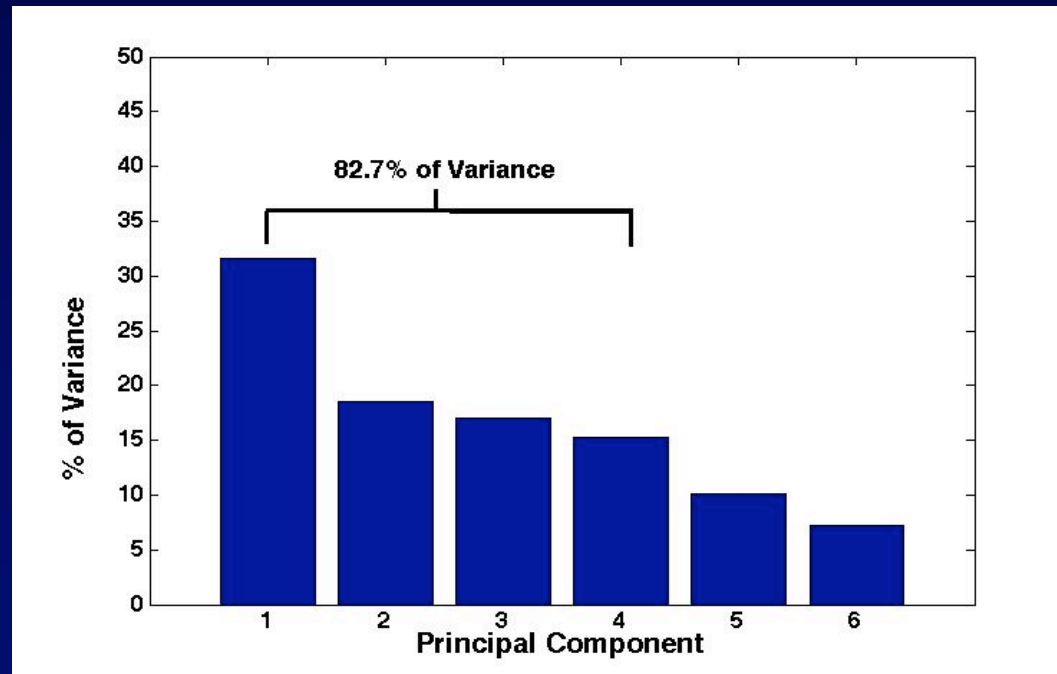
- averages scalar of quantities vs. tensor
- pixel-wise vs. whole-heart comparison

Principal Component Analysis

- reduces 10,000s to (N-1) DOF
- scalar measurements
- whole-heart comparison

Group of 11 mouse hearts

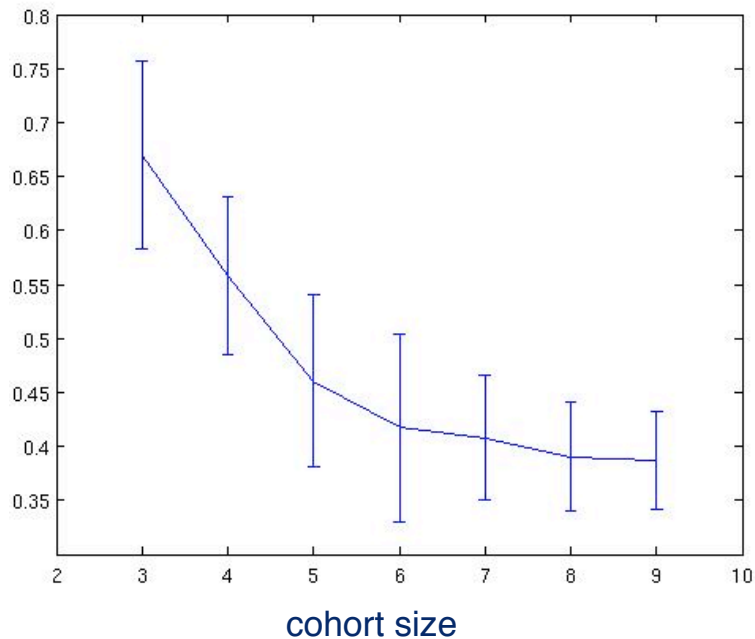
helix
angle



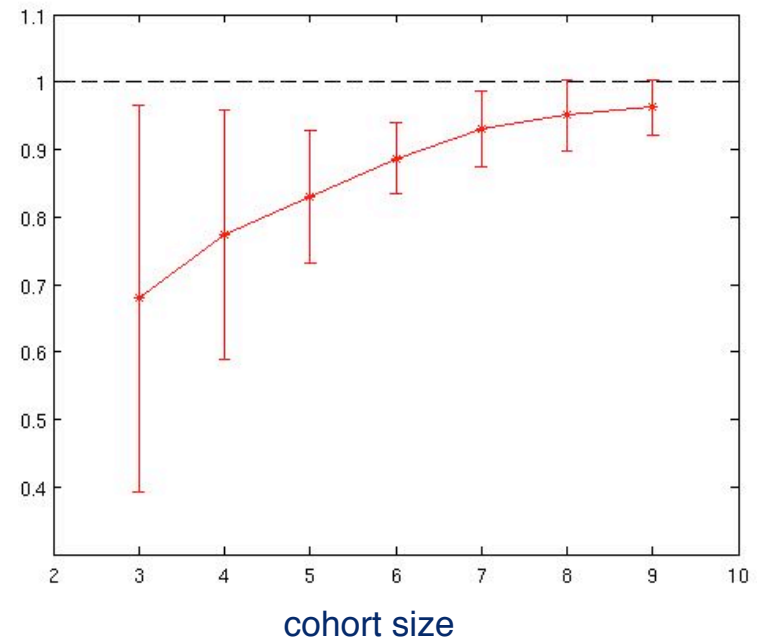
Statistical Power: First Helix Angle Component

Mean \pm SD of 20 sub-samples

Eigenvalue mean



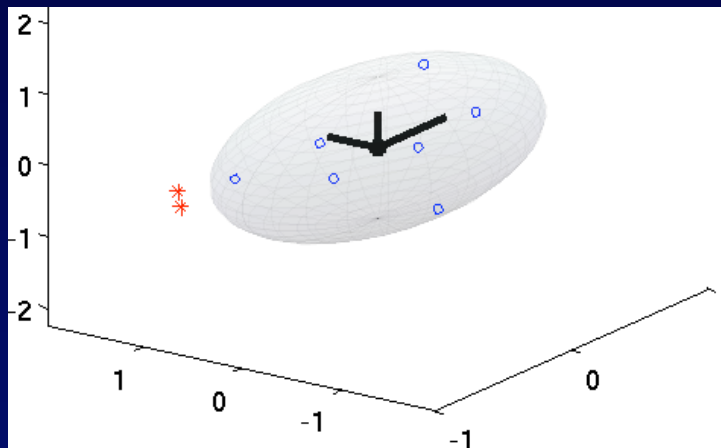
Eigenvector dot product



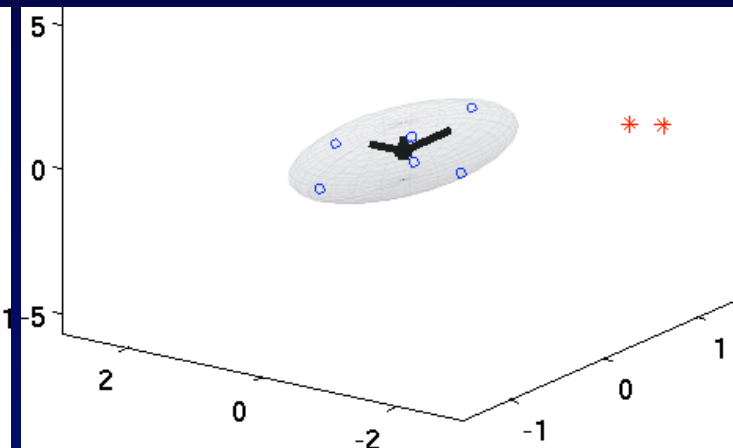
Detection of Hypertrophic Hearts

Collaborators: K. Padya, O. Smithes

α_H



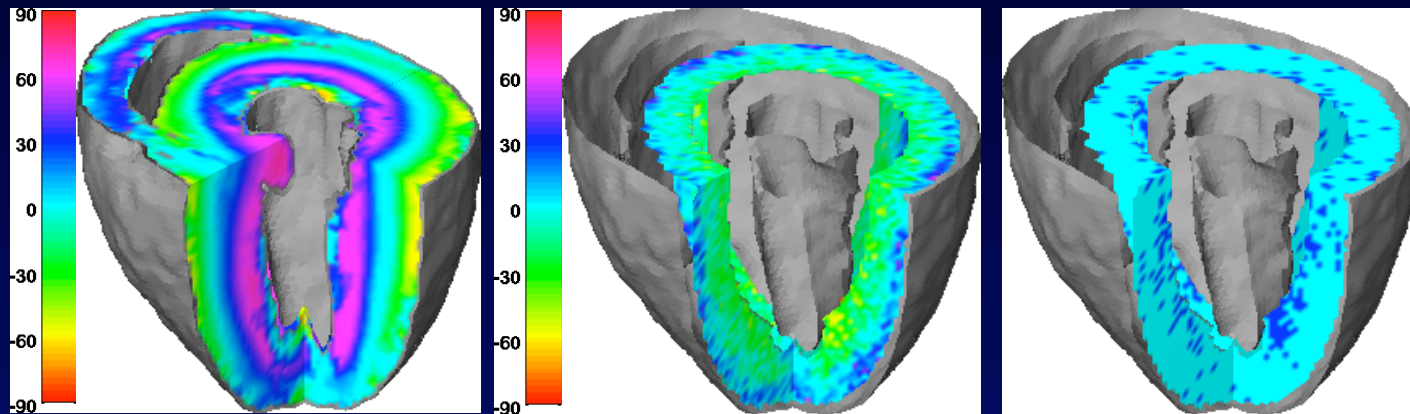
Anisotropy



Ellipses include 95% of data with $\pm 2SD$ in each dimension in 3D PCA space

Pixel-wise Comparison

Fiber Orientation Helix Angle



Group Mean

Difference

Significance

Whole-heart comparison can be advantageous

Conclusions

- Alternative to histology found
- Inter-species differences significant
- Intra-species variability tractable

Works in Progress

- Even more efficient DTI acquisitions
- Better in vivo cardiac DTI
- Vector or tensor-based statistics
- 4D and longitudinal atlases

Acknowledgments

Contributors

Sarang Joshi, Ph.D.

Zhi-Pei Liang, Ph.D.

Julius Guccione, Ph.D.

Yi Jiang, Ph.D.

Nilesh Mistry, Ph.D.

Wendy Shi

Lindsey Healy

Research Funding

NIH/NCRR

NIH/NHLBI

Whitaker

